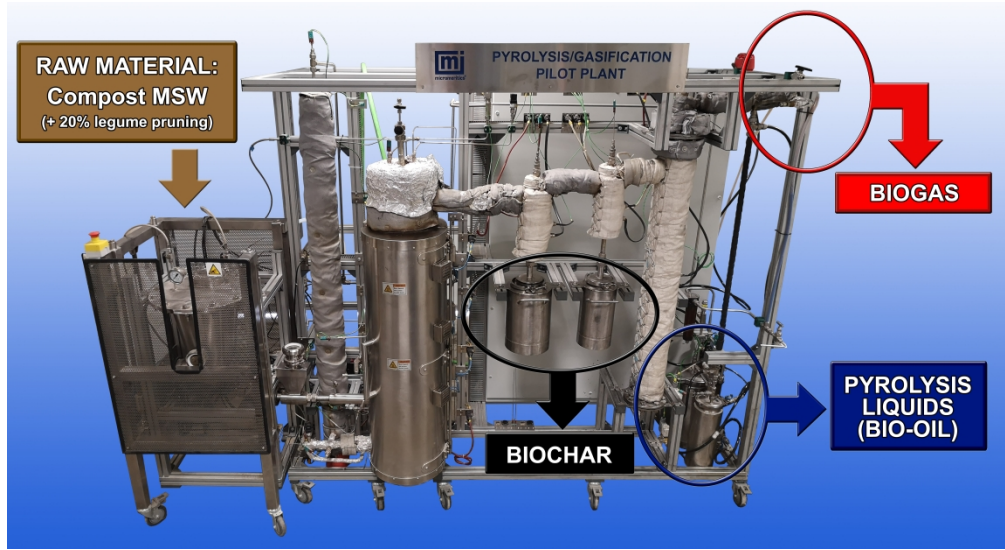


Pyrolysis of Municipal Solid Waste compost: pilot plant evaluation as a sustainable practise of waste management.

Journal:	<i>Waste Management & Research: The Journal for a Sustainable Circular Economy</i>
Manuscript ID	WMR-23-0322.R1
Manuscript Type:	Original Article
Date Submitted by the Author:	n/a
Complete List of Authors:	Palma, Alberto; University of Huelva, Department of Chemical Engineering, Physical Chemistry and Materials Science Clemente-Castro, Sergio; University of Huelva, Department of chemical engineering, physical chemistry and materials science. Ruiz-Montoya, Mercedes; University of Huelva, Department of chemical engineering, physical chemistry and materials science. Giráldez, Inmaculada; University of Huelva, Department of Chemistry "Prof. José Carlos Vílchez Martín" Díaz, Manuel Jesús; University of Huelva, Department of chemical engineering, physical chemistry and materials science.
Keywords:	pyrolysis, MSW compost, kinetic, GC/MS, biochar
Abstract:	To evaluate the potential of compost based on Municipal Solid Waste (MSW) and 20% legume pruning under a pyrolysis process, generated products, including solids (biochar), liquids (bio-oil) and gases (biogas), through experimentation in a pilot plant with a fluidised bed reactor at 450°C and gas chromatography/mass spectrometry (GC/MS) have been analysed. Also, the compost kinetic behaviour by thermogravimetric analysis (TGA), using Flynn-Wall-Ozawa method, has been investigated. Four different reaction zones, associated with lignocellulosic materials (hemicellulose, cellulose and lignin) with a first step for water evaporation, in TGA curve have been observed. A biochar with low stability and aromaticity, considering high and low O/C and H/C ratios, respectively, has been obtained. The obtained pyrolytic liquids contain a high concentration of phenolic compounds because of a significant presence of lignins and other high molecular weight compounds in the original material. Moreover, the generated biogas consists mainly of short-chain compounds such as alcohols, aldehydes and alkenes produced from hemicellulose, cellulose and proteins.

SCHOLARONE™
Manuscripts

1
2
3
4
5
6
7
8
9
10
11
12
13
14
15
16
17
18
19
20
21
22
23
24
25
26
27
28
29
30
31
32
33
34
35
36
37
38
39
40
41
42
43
44
45
46
47
48
49
50
51
52
53
54
55
56
57
58
59
60



Graphical abstract

4406x2413mm (38 x 38 DPI)

Highlights

- MSW Compost pyrolysis in pilot plant has been evaluated.
- The process kinetic to the pyrolysis of lignocellulosic materials could be assimilated.
- Compost can produce a low stability biochar in soil with low aromaticity.
- Bio-oil produced is composed of a highly phenolic fraction.
- Biogas of pyrolysis compost is a mixture of short-chain organic compounds.

For Peer Review

Pyrolysis of Municipal Solid Waste compost: pilot plant evaluation as a sustainable practise of waste management

A. Palma ^{*,a}, S. Clemente-Castro ^a, M. Ruiz-Montoya ^a, I. Giráldez ^b, M.J. Díaz ^a

Pro²TecS–Product Technology and Chemical Processes Research Centre

^aDepartment of Chemical Engineering, Physical Chemistry and Materials Science

^bDepartment of Chemistry “Prof. José Carlos Vilchez Martín”

University of Huelva. Campus “El Carmen”, 21071, Huelva (Spain)

*Corresponding author: alberto.palma@diq.uhu.es

Abstract

To evaluate the potential of compost based on Municipal Solid Waste (MSW) and 20% legume pruning under a pyrolysis process, generated products, including solids (biochar), liquids (bio-oil) and gases (non-condensable gases), through experimentation in a pilot plant with a fluidised bed reactor at 450 °C and gas chromatography/mass spectrometry (GC/MS) have been analysed. Also, the compost kinetic behaviour by thermogravimetric analysis (TGA), using Flynn-Wall-Ozawa method, has been investigated. Four different reaction zones, associated with lignocellulosic materials (hemicellulose, cellulose and lignin) with a first step for water evaporation, in TGA curve have been observed. A biochar with low stability and aromaticity, considering high and low O/C and H/C ratios, respectively, has been obtained. The obtained pyrolytic liquids contain a high concentration of phenolic compounds because of a significant presence of lignins and other high molecular weight compounds in the original material. Moreover, the generated non-condensable gases consist mainly of short-chain compounds such as alcohols, aldehydes and alkenes produced from hemicellulose, cellulose and proteins.

Keywords: pyrolysis; MSW compost; kinetic; GC/MS; biochar.

1. Introduction

It has been widely recognised that inadequate treatment of organic waste can lead to significant environmental and health problems. In this respect, the beneficial properties of compost both as a suitable solution for the treatment and sanitation of organic waste and its subsequent use in agriculture (both technically and economically) have been extensively demonstrated (Rashid and Shahzad, 2021). Despite the problems that inadequate management, mainly due to the odours emitted (Delgado-Rodríguez et al., 2011) can cause.

The quality of the final compost will depend significantly on the nature and quality of the waste to be composted. However, the process parameters are also involved in the degradation to which the organic compounds are subjected during composting. Therefore, a high variability of quality in the produced compost can be ascertained, and quality standards for its use in agriculture must be applied (Hameed et al., 2021). However, in addition to the traditional uses of compost, new uses and organo-mineral formulations (Fachini et al., 2021) are being developed.

In the EU-28 (28 EU Member States) approximately 88 million tonnes/year of food are wasted. About 20% of the food produced represents this value. Because of various problems, including lack of segregated sorting and impurities, only 17% of this municipal waste can be properly composted and/or digested (EEA, 2020). Therefore, a high proportion of composted Municipal Solid Waste (MSW) is not of a quality suitable for direct use in agriculture.

Consequently, various ways of valorization of this compost of low agronomic quality, apart from the alternative uses that are already being used, such as the recovery of degraded areas (mines, quarries, landfills), forestry crops, etc.,

1
2
3 should be explored. Therefore, enhancing the valorisation pathways of these
4 materials to improve the management of these wastes should be developed.
5

6
7 Thermochemical processes, due to the wide range of products (solid, liquid and
8 gaseous) and/or energy generated, are an alternative to be considered for the
9 valorisation of organic materials. Among these, combustion (with an excess of
10 oxygen over that required according to stoichiometry), gasification (with a deficit
11 of oxygen over that required according to stoichiometry) and pyrolysis (without
12 oxygen) can be noted (Beis et al., 2002).
13
14
15
16
17
18
19
20

21 In this sense, pyrolytic processes as a source of new high value-added products
22 from compost can be highlighted. During composting, organic compounds are
23 generally degraded or directly mineralized, although a portion of the high
24 molecular weight compounds present in the original material increase the degree
25 of aromaticity in the resulting composted compounds. Also, an increase in the
26 mass degradation above 600 °C as the composting time increases (Díaz et al.,
27 2021) is produced. Thus, the composting process significantly alters the
28 distribution of chemical compounds and may result in products that may not be
29 produced during pyrolysis of other sources of organic compounds.
30
31
32
33
34
35
36
37
38
39
40
41

42 Among these innovative materials from compost by pyrolysis, Qian et al. (2007)
43 and Finney et al. (2009) used compost, from livestock manure and mushroom
44 industry residues, respectively, as raw material for the production of biochar.
45 Also, the use of composts, in the pyrolysis process, as a potential feedstocks for
46 bio-oil production has been studied by Garrido et al. (2012) and Giwa et al.
47 (2018).
48
49
50
51
52
53
54
55

56 The general objective of this work is to study the products generated (biochar,
57 pyrolytic liquids and volatile organic compounds) during the pyrolysis of MSW
58
59
60

compost with 20% pruning residues. Also, the kinetics of the reactions produced during the pyrolysis of these composts has been studied.

2. Materials and Methods

2.1. MSW composition

The different components of MSW can be classified into three main groups: fermentable (food waste), combustible (paper, cardboard, plastics, rubber, textiles, wood, etc.), and inert (metals, glass, etc.). The composition of MSW is highly variable and depends on factors such as the standard of living, lifestyle of the population, and the time of year. The composition of the MSW composted in this study is shown in Figure 1.

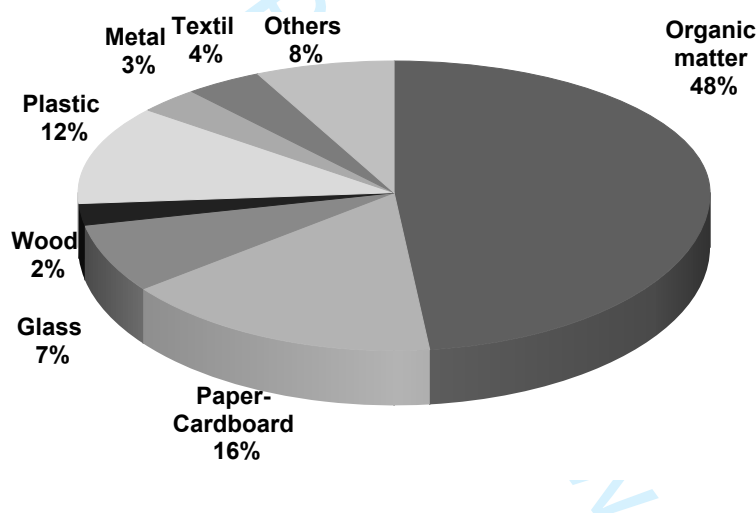


Figure 1. MSW composition.

2.2. Compost characteristics

Non-selective Municipal Solid Waste Compost (MSWC) from Villarrasa (Huelva - Spain) urban waste treatment plant is used in this study. Prior to composting the main treatment involves trammel-screening (8 cm), metal electromagnetic separation and manual separation of plastics. To improve internal aeration in composting piles, 20% of bulking material (legume pruning of *Leucaena*

leucocephala), before the composting process, have been added. The non-degraded fraction of this material was separated by screening at the end of the composting process. The most relevant chemical characteristics of the final compost are reported in Table 1.

Property	Units	Compost (after 40 days)
pH (1:5 extract)		7.8 ± 1.2
EC (1:5 extract)	dS m ⁻¹	8.5 ± 1.1
Organic Matter	g kg ⁻¹	593 ± 32
Kjeldahl-N	g kg ⁻¹	12.3 ± 3.5
Ash	g kg ⁻¹	35.4 ± 4.7
C/N		26.6
Moisture	%	0.6

^a Determined in MSW <5 mm and free of impurities

^b Mean values and standard deviations were calculated from the triplicates

Table 1. Relevant characteristics of used MSWC^a (average ± standard deviation)^b

2.3. Processing of the samples by pyrolysis with TGA

The dried compost samples, with an initial average diameter of 50 mm, were milled into particles of smaller size (1-2 mm). The final particles were stored without contact with air moisture. Thermochemical decomposition behavior was evaluated using a thermo-gravimetric analyzer (TGA) (Mettler Toledo TGA/DSC1 STARe System). TGA experiments heating 10-25 mg samples from 25 °C to 850 °C, at four heating rates (5, 10, 15 and 20 °C min⁻¹) under nitrogen flow rate of 20 cm³ min⁻¹ have been performed. The obtained thermo-gravimetric analysis data

1
2
3 for any changes in the thermo-chemical decomposition behavior have been
4
5 studied.
6

7 8 **2.4. Pilot plant pyrolysis** 9

10 A laboratory-scale fluidized bed reactor (PID Eng&Tech Micromeritics) has been
11 employed. An operating temperature of 450 °C has been used. 30 L min⁻¹ of
12 nitrogen (twice the minimum fluidization rate) has been used, with a constant
13 pressure difference of 33 mbar.
14
15
16
17

18 A gas cleaning system at the reactor outlet has been installed. This system
19 consists of two cyclones (CY1 for particles >20µm and CY2 for particles >5µm)
20 that have been connected in series. Downstream, a heat exchanger (400°C to
21 90°C), controlled by a single valve, is used to regulate the inflow of the coolant
22 fluid (water 20°C) into the heat exchanger. Pyrolytic liquids in a cooling vessel
23 (first condenser (CD1) at 63 °C), located at the bottom of the heat exchanger
24 have been collected. Water and other condensed liquids are retained in a second
25 condenser (CD2) (30°C). Finally, the product gases pass through coalescing
26 filters before sampling and finally into a scrubber (23°C).
27
28
29
30
31
32
33
34
35
36
37
38
39

40 **2.5. Pyrolytic liquid analysis** 41

42 An aliquot to pyrolytic liquid has been extracted with water (1:10 ratio), vortexed
43 30 s and centrifugation for 20 min at 5000 rpm. Then, 1 mL the water-insoluble
44 fraction was extracted with diethyl ether (DEE) (3 x 1 mL). After extraction, an
45 aliquot DEE extract (500 µL) has been dried under nitrogen and 50 µL of both
46 pyridine and BSTFA/TMCS (90:10) were added following incubated for 30 min at
47 60°C. Then, TMS derivative extracts were diluted (1:10) with CHCl₃ and 1 µL was
48 injected into GC-MS/MS (GCMSQP8030 Ultra System, Shimadzu, Japan). TMS
49 derivative compounds were separated by a HP-5 MS column (60 m, 0.25 mm I.D.).
50
51
52
53
54
55
56
57
58
59
60

0.25 μm film thickness, J&W Scientific, Agilent Technologies, USA). The GC oven was programmed: 50 $^{\circ}\text{C}$ for 2 min, ramped at 8 $^{\circ}\text{C min}^{-1}$ to 280 $^{\circ}\text{C}$, held for 2 min. A second ramp rate was performed of 50 $^{\circ}\text{C min}^{-1}$ until a final temperature of 300 $^{\circ}\text{C}$ was reached and held for 2 min. Helium at constant flow rate of 1.20 mL min^{-1} was used as the carrier gas. The temperatures of the injection port (split mode 10:1), transfer line and ion source were maintained at 250, 280 and 230 $^{\circ}\text{C}$, respectively. The mass spectrometer was operated in scan mode (50-800 m z^{-1}). TMS derivative compounds were identified by comparison of the mass spectra with those of the database of NIST11 library. For control and data analysis, GCMS Postrun Analysis Shimadzu was used. The MS was turned with perfluorotributylamine (PFTBA).

2.6. Biochar analysis

Gross Calorific Value (constant volume) following the standards "CEN/TS 14918:2005 (E) Solid Biofuels - Method for the determination of the calorific value" and UNE 164001 EX have been determined. Automatic Isoperibol Calorimeter Parr 6300 has been used. Total carbon, hydrogen and sulphur simultaneously in a ELTRA Carbon/Hydrogen/Sulfur Analyzer CHS-580A (ELTRA GmbH, Germany) have been determined. The standard guidelines for the determination of carbon, hydrogen (EN 15104:2011) and sulfur (EN 15289:2011) have been followed. Moreover, oxygen content by difference (CEN/TS 14961, 2005) has been also calculated. According to ISO 10390:2005, biochar was air-dried and crushed into fine particles (<2 mm). Then, the sample was soaked with 0.01 M CaCl_2 at a 1:5 solid/water ratio for 1 h with agitation.

1
2
3 After still standing for 1 h, the slurry was then measured for pH using a pH-meter
4 GLP 21 (Crison Instruments, S.A.).
5
6

7 **2.7. Volatile compounds gas samples analysis by pyrolysis TD/GC-MS**

8
9
10 Volatile compounds gas samples from the pilot plant pyrolysis process at 350 and
11 550°C (corresponding to higher temperatures than the degradation maxima found
12 in the TGA curves) were collected in fritted glass TD tubes (Supelco, Bellefonte,
13 PA; O.D.: 6.35 mm; length: 88.9 mm) for 1.5 min. Tubes containing 100 mg of
14 Tenax® TA (80-100 mesh purchased from Supelco, Bellefonte, PA) packed in
15 layers of silanized glass wool. TD tubes after sampling have been analyzed using
16 TD/GC-MS. TD was used to release the captured volatile compounds from the
17 tube sorbent material onto the GC/MS for identification and quantification. TD
18 was carried out by use of thermal desorption system unit (TD-20, Shimadzu,
19 Japan) fitted with a HP-5 MS column (60 m, 0.25 mm I.D. 0.25 µm film thickness,
20 J&W Scientific, Agilent Technologies, USA) and involved 2 steps: tube desorption
21 and trap desorption. The mass spectrometer was operated in scan mode (41-450
22 m z⁻¹). Volatile organic compounds were identified by comparison of the mass
23 spectra with those of in the database of NIST11 library using as internal standard
24 1-bromo-3-chlorobenzene (BCB). For control and data analysis, the GCMS
25 Postrun Analysis Shimadzu was used. The MS was turned with
26 perfluorotributylamine (PFTBA).
27
28
29
30
31
32
33
34
35
36
37
38
39
40
41
42
43
44
45
46
47
48

49 **2.8. Kinetic analysis by Flynn-Wall-Ozawa method**

50
51 The activation energy of pyrolysis reactions in lignocellulosic materials has been
52 studied by several different mathematical methods. In this regard, the use of
53 isoconversional methods for the determination of pyrolysis kinetics has been
54 successfully documented (Açıklalın and Gözke, 2021). Moreover, according to the
55
56
57
58
59
60

1
2
3 results obtained by Fernández-López et al. (2016) and Palma et al. (2020), this
4 model has been satisfactorily tested in different composts. Moreover, Gunasee
5 et al. (2016) have demonstrated that this TGA-based experimental methodology
6 could be suitable for revealing synergistic reactions during co-pyrolysis of
7 different MSW.
8
9

10
11
12 For a given reaction, the activation energy should be a constant value throughout
13 the weight loss region, so changes in these values imply degradation of other
14 compounds. In the present study the activation energy values for the degradation
15 process using the Flynn-Wall-Ozawa (FWO) isoconversional method (Flynn and
16 Wall, 1966; Ozawa, 1965) defined by Eq. 1 have been determined. This method
17 for determination of the E_a values without any knowledge of its mechanisms (El-
18 Sayed and Mostafa, 2015) can be used.
19
20
21
22
23
24
25
26
27
28
29

$$\ln(\beta) = \ln\left(\frac{A E_a}{R g(\alpha)}\right) - 2.315 - 0.4567 \frac{E_a}{RT} \quad (\text{Eq. 1})$$

30
31
32 where β is the heating rate, A is the pre-exponential factor, $g(\alpha)$ is a function of
33 the conversion, E_a is the activation energy and R is the gas constant.
34
35
36
37

38 Therefore, for different heating rates (β) and a given degree of conversion (α), a
39 linear relationship is observed by plotting of natural logarithm of heating rates (\ln
40 β), versus $(1/T)$ obtained from thermal curves recorded at different heating rates
41 will be a straight line whose slope $(-0.4567 (E_a/RT))$ will calculate the activation
42 energy.
43
44
45
46
47
48

49 **3. Result and Discussion**

50 **3.1. Compost TGA analysis**

51
52 Thermograms of compost (TGA) and their derivative (DTG) with respect to
53 temperature corresponding to pyrolytic decomposition of MSWC, at $20^\circ\text{C min}^{-1}$
54
55
56
57
58
59
60

are shown in Figure 2 (for the kinetic parameters calculation four thermograms, at four heating rates 5, 10, 15 and 20°C min⁻¹, have been carried out. To show the evolution only the last thermogram has been displayed. In this form, the mass loss profile (TGA) and its derivative curve (DTG) obtained by thermogravimetric analysis are shown in Figure 2.

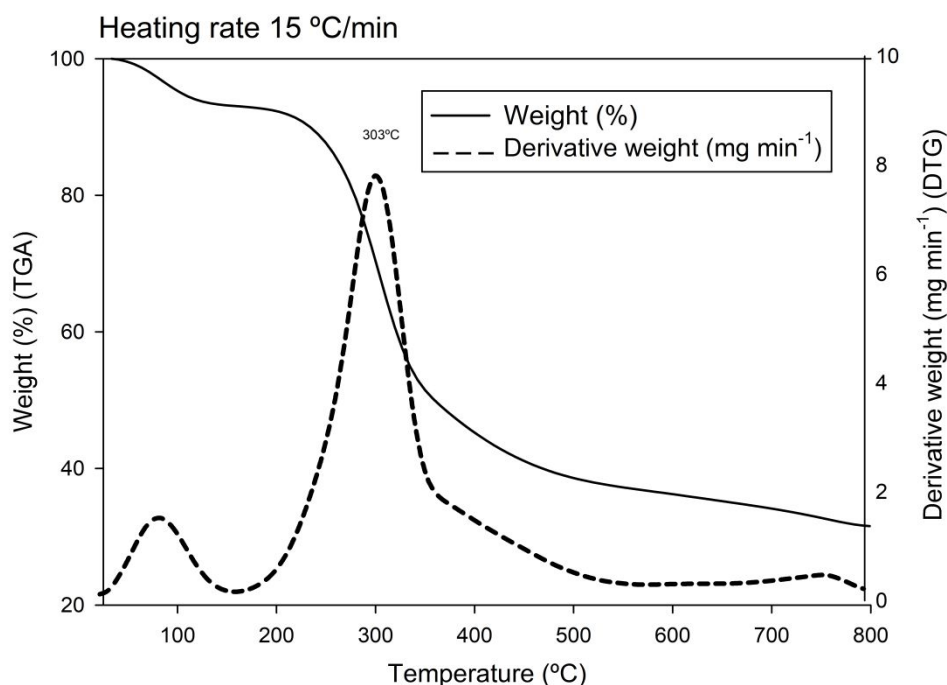


Figure 2. TGA and DTG correspond to MSW Compost pyrolytic degradation at 20°C min⁻¹.

The figure shows the typical evolution described by different researchers (Dhyani et al., 2018). Similar to what was observed by López-González et al. (2014) in the pyrolysis process of manure compost, a thermochemical behavior similar to that of lignocellulosic biomass can be observed. In this evolution the three main phases in the thermal degradation of compost: phase I between 25 and 120 °C; phase II between 200 °C and 400 °C and phase III between 400 °C and 700 °C can be observed. The peak found (DTG) in the first phase (<200°C) corresponds

1
2
3 to the dehydration process of the compost sample although some authors
4 indicate that decarboxylation may also occur in labile compounds (Pietro and
5 Paola, 2004). The main peak (DTG) in the second phase (200-350 °C) can be
6 identified and a weight loss over 44% at this stage can be calculated. This second
7 peak to the thermal degradation of simple organic matter and semi-volatile
8 compounds such as hemicelluloses, cellulose, degradation of aliphatic structures
9 and microbial cell walls can be associated (Baigorri et al., 2009). The data
10 reported in this study are similar to those presented by Sánchez-Silva et al.
11 (2012) for which a significant weight loss between 210 and 373 °C has been
12 reported. This implies a lower temperature range than that found for the different
13 lignocellulosic biomasses, which are usually between 200 and 450 °C. This fact
14 may be due to the lower lignin content (which is the most thermally stable
15 compound) in compost compared to lignocellulosic biomass. The third phase
16 (350-600 °C, shoulder in the DTG) to the degradation of aromatic structures and
17 organic polymers such as lignin, or synthesized during the compost stabilization
18 process has been associated (Dhyani et al., 2018; Soobhany et al., 2017).
19 Additionally, the peak found at temperatures above 600 °C to the volatilization of
20 the produced biochar and inorganic components (nitrates and carbonates, etc.)
21 has been attributed (Parthasarathy et al., 2021).

22
23
24
25
26
27
28
29
30
31
32
33
34
35
36
37
38
39
40
41
42
43
44
45
46
47
48
49
50
51
52
53
54
55
56
57
58
59
60
The optimum temperature to obtain the maximum yield will vary depending on
the feedstock. According to the TGA evolution, with a reactor temperature of 450
°C a degradation of the organic matter in the studied composts without
volatilization of the inorganic components can be assured. In this sense, Buah et
al. (2007), Agirre et al. (2013), Ansah et al. (2016) experiences of pyrolysis of
MSW between 400 and 550 °C have carried out and approximately, between

400-600 °C the optimal temperature range for most lignocellulosic materials has been published (Tagade et al., 2021). Nevertheless, within the optimum range, the operating temperature not only modifies the bio-oil yield but also changes its composition. In this regard, it has been published that under lower temperatures more carbon can be produced while, under temperatures between 500 °C and 550 °C, higher bio-oil yields can be found. Also, at temperatures above 600 °C, the bio-oil yield may decrease and an increase of non-condensable gases may be found (Ansari et al., 2018).

3.2. Compost pyrolysis kinetics

Table 2 shows the results of the application of the FWO method. In this regard, Palma et al. (2020) in a study of the pyrolysis of MSW compost, concluded that adjusting the pyrolysis of MSW compost to first-order kinetics appears to be a suitable approach. A similar trend to that found by other researchers in lignocellulosic biomass (Açıklan and Gözke, 2021) has been found in the evolution of the Activation Energy of compost. This similar behavior by other authors has been previously described (Fernández-López et al., 2016). Thus, an increase up to values close to 200 kJ mol⁻¹ has been found at 20% ($\alpha=0.20$) conversion.

Conversion (α)	Ea (kJ mol ⁻¹)	log(A) (log s ⁻¹)
0.2	211.9	20.6
0.3	191.4	19.7
0.4	222.3	20.0
0.5	301.6	21.1
0.6	150.2	21.5
0.7	85.4	23.3

Table 2. Calculated Activation energy of MSWC under conversion degree (α) by using Flynn-Wall-Ozawa method.

The 20% conversion occurs at 300 °C, at this temperature the degradation of hemicelluloses and cellulose begins. In this respect, Collard and Blin (2014) showed that cellulose pyrolytic degradation occurs mainly between 300 and 400 °C. Also, proteins also decompose at such temperatures (Kebelmann et al., 2013). During this process, E_a remains at similar values up to 50% conversion ($\alpha=0.5$), which approximately corresponds to 450°C. At this point, according to Soobhany et al. (2017), with the degradation of aromatic structures, depolymerization of lignin and other organic polymers synthesized during the compost stabilization process (humic and fulvic substances), have been associated and, this fact, can lead to an increase in E_a values to 301.6 kJ mol⁻¹. In this sense, the drop in E_a at the lower values of this parameter for lignin-derived compounds (34.94-122.24 KJ mol⁻¹) (Soh et al., 2019), with respect to those found for cellulosic derivatives (340-360) (Huang et al., 2011), may be due.

The calculated activation energy values are in the range found by other authors (60-600 kJ mol⁻¹) (Fernández-López et al., 2016; Palma et al., 2020). Moreover, Palma et al. (2020) have studied the pyrolysis of MSW compost under two different composting conditions (different aeration and moisture) finding activation energy values in the range of 57.78-581.69 kJ mol⁻¹.

Finally, after the depolymerization processes of the different compounds formed during composting, a drop in E_a has been calculated (to values similar to 150 kJ mol⁻¹) for $\alpha>0.6$, which can be attributed to the volatilization of residual carbon in

1
2
3 the compost (Dhyani et al., 2018) since the temperatures at which it takes place
4 are higher than 600 °C.
5

6
7 The velocity constant, following the Arrhenius Equation (basis of the Flynn-Wall-
8 Ozawa model) can be expressed as (Eq. 2).
9

$$10 \quad k(T) = A \cdot e^{\frac{-E_a}{R \cdot T}} \quad (\text{Eq. 2})$$

11
12 where T is Temperature 450 °C (723 K), R=8.314472 J mol⁻¹ K⁻¹. Substituting the
13 maximum values (Table 2) of Ea (301.6 kJ mol⁻¹) and A (21.1 s⁻¹), we can obtain
14 a velocity constant: k=21.1 mol s⁻¹. Therefore, given the high level of degradation
15 that, under the proposed conditions, takes place. At low material addition levels,
16 to the fluidized bed reactor, a complete conversion can be ensured.
17
18
19
20
21
22
23
24
25

26 **3.3. Material Balance**

27
28 The material was introduced into the pyrolytic reactor at a rate of 1000 g h⁻¹. The
29 operating time was 30 min, thus, 500 g (6% moisture) has been processed.
30

31
32 The biochar yields were 83.55 g (16.71 %) and 40.25 g (8.05%) for cyclones CY1
33 and CY2, respectively, with moisture contents of 0.83% and 0.18%, respectively.
34

35
36 This means almost 25% yield in biochar. In this regard, comparable values for
37 different biomasses by Boateng et al. (2012) (17-28%), Jaroenkhasemmesuk
38 and Tippayawong (2015) (30%) and Larina and Zaichenko (2018) (35%), under
39 temperatures similar to the studied ones, have been found. Generally, moisture
40 contents lower than 11% in raw materials have little influence on biochar yield (Di
41 Blasi et al., 2000) because a high initial moisture content of the feedstock and a
42 slow heating rate may result in an incomplete devolatilization of the biochar.
43
44
45
46
47
48
49
50
51
52

53
54 In the condensable fraction of pyrolysis (pyrolytic liquids), 162.2 g (32.44%) and
55 18.35 g (3.67%) yields in condensers CD1 and CD2, respectively, have been
56 found. This means 36.11% yield in condensable fraction. Comparable values
57
58
59
60

1
2
3 have been found, by Boateng et al. (2012) (10-45%) and Jaroenkhasemmesuk
4 and Tippayawong (2015) (30%) for different biomasses, although lower than
5 those found by Mohan et al. (2006) (60-75%). According to Ferreira (2000),
6 almost 100% of the intrinsic water in the compost (8%) is responsible for the major
7 part and composition of the liquid found in condensers.
8

9
10
11
12
13
14 Over 64% increment in water content with respect to the initial water content has
15 been found. This may be due to the reaction that, at the process temperatures,
16 has been taking place between the oxygenated compounds in the compost (being
17 the product of biooxidative reactions) and the hydrogen released during the
18 pyrolytic degradation reactions, resulting in a high water yield.
19

20
21
22
23
24
25
26 The measured non-condensable gases was 171.6 g (36.32%) with a moisture
27 content of 0.12%. Thus, a total yield in the balance of 95% was calculated. A wide
28 range 27-73% on bibliography (Boateng et al., 2012) have been found because
29 the condensation time and conditions significantly vary the amount of gas
30 produced. In this regard, a value similar to this study by Jaroenkhasemmesuk
31 and Tippayawong (2015) (40%) has been found. Although a value higher than
32 that found by Larina and Zaichenko (2018) (15%) and lower than those found by
33 Mohan et al. (2006) (60-75%), has been calculated. The rest at different process
34 points had to be deposited.
35
36
37
38
39
40
41
42
43
44
45

46 **3.4. Biochar analysis**

47
48
49 The amount of biochar obtained 35.6 ± 3.2 (w.t.) is slightly higher than that found
50 by Ghorbel et al. (2015) who showed a yield of 31% in biochar from farm breeding
51 compost and similar to the yields obtained in biomass pyrolysis (25-40%) at the
52 reaction temperature (Ghodake et al., 2021). The elemental composition of the
53 resulting biochar in Table 3 is shown. Moreover, the ash content of the resulting
54
55
56
57
58
59
60

biochars increased significantly with respect to the feedstock ash due to the loss of organic matter which, during the pyrolysis process, passes into the gas phase. Similarly, the carbon content in the biochar increased by 8.6% with respect to the original compost. The progressive concentration of carbon and minerals during volatilization produced by increasing temperatures can cause this process.

	C (%)	H (%)	O (%)	S (%)
Cyclon 1 (CY1)	46.6 ± 2.7	1.62 ± 0.3	51.2 ± 2.3	0.54 ± 0.1
Cyclon 2 (CY2)	48.7 ± 1.9	1.84 ± 0.5	48.9 ± 2.0	0.51 ± 0.1

^a Mean values and standard deviations were calculated from the triplicates

Table 3. Chemical characteristics of obtained biochar^a.

The H/C and O/C ratios to estimate the stability of biochar in soil are commonly used. O/C ratio may be a suitable indicator of biochar stability and may inform about the general polarity of the material (Shakya and Agarwal, 2017). The O/C ratio the abundance of polar oxygen-containing surface functional groups in biochar can indicate (Rangabhashiyam and Balasubramanian, 2019). Therefore, high values indicate a higher polarity of functional groups. Alternatively, low O/C ratios, because the adsorption mechanism shifts from being mainly based on ion exchange to physisorption (Ahmad et al., 2012), low adsorption capacity may indicate due to the weaker nature of physisorption. In this study, high O/C ratios >0.6 (0.9-1.0) have been found and these data may be indicative of a product that is not very stable in soil and therefore, low stability of the biochar produced can be assumed.

On the other hand, H/C ratio the aromaticity and stability of the biochar (Wei et al., 2020; Xiao et al., 2016) may indicate. Low values for this parameter have been found, therefore a low aromaticity can be shown.

These data, with respect to different biomasses, are shown in Figure 3. Differences, mainly in the H/C ratio, with respect to other biochar have been found. This may be due to the loss of aromatic structures that during composting (Joyce et al., 1998), due to the previous microbiological action, has taken place and that may have caused the differences with respect to other biochar from original biomass.

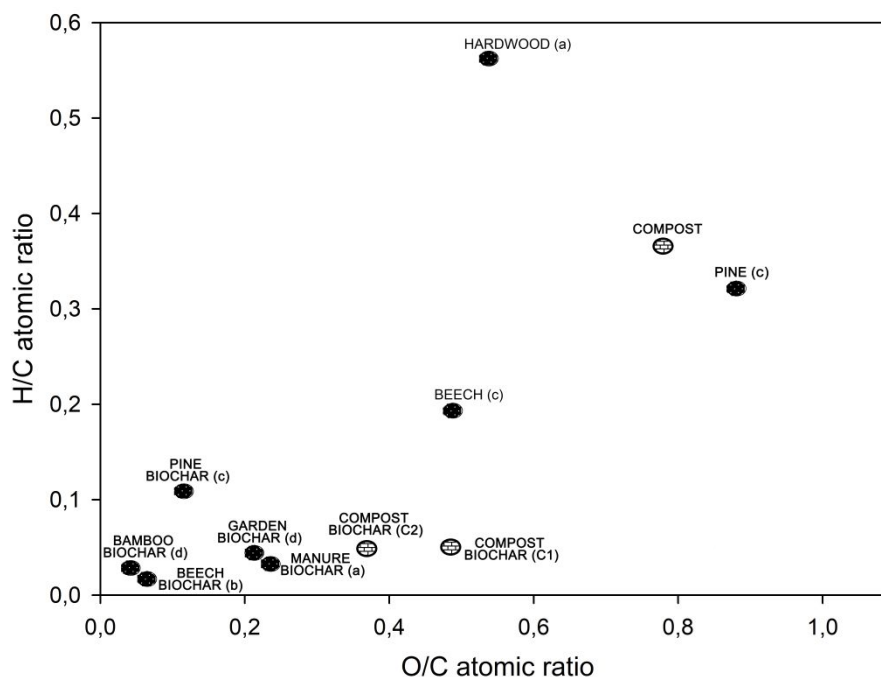


Figure 3. Van Krevelen graph (H/C vs O/C atomic ratio) for the obtained compost biochar with respect to other raw materials (^aFabbri et al. (2012); ^bMorin et al. (2016); ^cGuizani et al. (2017); ^dDang et al. (2021).

Low values of gross heating, 14.18 and 18.56 MJ kg⁻¹ for C1 and C2 samples, respectively, have been found. Values similar to 25-30 MJ kg⁻¹ in biochars from

1
2
3 different feedstocks have been found (Jiang et al., 2018; Tsai et al., 2018), but
4
5 higher than those found by Mierzwa-Hersztek et al. (2019), in the range of 11-12
6
7 MJ kg⁻¹ for sawdust, wheat straw, and miscanthus straw. In this regard, Tripathi
8
9 et al. (2016) showed that the calorific value of biochar is directly proportional to
10
11 the process temperature and inversely proportional to the H/C and O/C molar
12
13 ratios. The obtained data supports the conclusions drawn by these authors.
14
15

16 Alkalinity is one of the most influential properties of biochar, because changes in
17
18 pH have large impact on many soil processes (Fidel et al., 2017). In this study,
19
20 values of 12.04 and 12.37 have been found for C1 and C2, respectively. In this
21
22 regard, Li et al. (2013) and Fidel et al. (2017) showed values between 5.5-10.3
23
24 depending on the biochar feedstock and pyrolysis conditions. The values found
25
26 in biochar from MSW compost, are higher than those found by the previous
27
28 authors. This fact may be due to the high amount of basic salts usually found in
29
30 MSW compost (Xie et al., 2020) that give rise to a basic pH already in the original
31
32 compost and that are concentrated by the pyrolysis process in the biochar
33
34 obtained since the process conditions (450°C) do not cause the volatilization of
35
36 these salts.
37
38
39
40

41 42 **3.5. Bio-oil GC/MS analysis**

43
44 The bio-oil obtained from the pyrolysis of compost at 450 °C for 30 min in a
45
46 fluidized bed reactor was analyzed by GC-MS and are shown in Table 4. Since
47
48 the compost is formed mainly by lignocellulosic material composed of cellulose,
49
50 hemicellulose and lignin, the pyrolysis products are derived from these
51
52 components in different proportions. Numerous chemical compounds have been
53
54 obtained in bio-oils but the complete identification is complex, with 24 of the most
55
56 important compounds identified and studied in depth.
57
58
59
60

The main cellulose decomposition compound in compost pyrolysis as furan-2-ylmethanol (3.3%) and as nitrogenous product is found 5-(hydroxymethyl)-1-methylpyrrolidin-2-one (2.4%) have been found. As shown in Table 4, the phenolic compounds typical in lignin disintegration, such as methylphenols (12.7%), 2-methoxyphenol, better known as guaiacol (6.9%), 4-methylbenzene-1,2-diol (5.7%) or 3-(2-hydroxyethyl)phenol (6.4%) have been found among many others, assuming more than 80% of the total of degraded products.

The low concentration of short-chain compounds common of the fragmentation of cellulose and hemicellulose such as carbohydrates highlighting the levoglucosan in the pyrolytic liquids (Kim et al., 2013) compared to untreated lignocellulosic biomass reveals the decomposition of these components in the composting process, making more complex lignin compounds attract attention to a greater extent.

Compounds	Formula	MS	RT (min)	Area (%)
<i>Ethane-1,2-diol</i>	C ₂ H ₆ O ₂	62.07	12.591	2.45
<i>Furan-2-ylmethanol</i>	C ₅ H ₆ O ₂	98.10	12.904	3.29
<i>Phenol</i>	C ₆ H ₆ O	94.11	14.288	6.32
<i>5-(hydroxymethyl)-1-methylpyrrolidin-2-one</i>	C ₆ H ₁₁ NO ₂	129.16	15.653	2.44
<i>2-methylphenol</i>	C ₇ H ₈ O	108.14	16.050	3.30
<i>3-methylphenol</i>	C ₇ H ₈ O	108.14	16.220	4.58
<i>4-methylphenol</i>	C ₇ H ₈ O	108.14	16.444	4.82
<i>3-methylcyclohex-1-en-1-ol</i>	C ₇ H ₁₂ O	112.17	17.558	6.19
<i>2-methoxyphenol</i>	C ₇ H ₈ O ₂	124.14	18.088	6.29
<i>3-ethylphenol</i>	C ₈ H ₁₀ O	122.16	18.272	2.11
<i>benzene-1,3,5-triol</i>	C ₆ H ₆ O ₃	126.11	19.040	3.08
<i>2-methoxy-5-methylphenol</i>	C ₈ H ₁₀ O ₂	138.16	19.862	3.34
<i>benzene-1,4-diol</i>	C ₆ H ₆ O ₂	110.11	19.938	3.73
<i>3-methylbenzene-1,2-diol</i>	C ₇ H ₈ O ₂	124.12	21.265	2.68
<i>methyl 3-hydroxybenzoate</i>	C ₈ H ₈ O ₃	152.15	21.321	5.36
<i>2,6-dimethoxyphenol</i>	C ₈ H ₁₀ O ₃	154.16	21.450	3.26

<i>4-methylbenzene-1,2-diol</i>	$C_7H_8O_2$	124.14	21.528	5.69
<i>1-(2-hydroxyphenyl)propan-1-one</i>	$C_9H_{10}O_2$	150.17	22.122	5.06
<i>3-(2-hydroxyethyl)phenol</i>	$C_8H_{10}O_2$	138.16	22.528	6.39
<i>2-methoxy-4-propylphenol</i>	$C_{10}H_{14}O_2$	166.22	22.685	4.62
<i>1-(2-hydroxy-6-methoxyphenyl)ethanone</i>	$C_9H_{10}O_3$	166.17	23.553	4.67
<i>2-methoxy-4-prop-2-enylphenol</i>	$C_{10}H_{12}O_2$	164.20	23.861	2.15
<i>1-(4-hydroxy-3-methoxyphenyl)ethanone</i>	$C_9H_{10}O_3$	166.17	24.359	6.01
<i>4-(3-hydroxypropyl)-2-methoxyphenol</i>	$C_{10}H_{14}O_3$	182.22	28.106	2.15

Table 4. Main compounds found by GC/MS in bio-oil of MSW compost pyrolysis at 450°C.

3.6. Non-condensable gases GC/MS analysis

The volatile organic pyrolysis products that are found in a small proportion mixed with mainly nitrogen and other light gases detected by GC/MS are shown in Table 5. In this case, the non-condensable gases contain compounds derived from hemicellulose and cellulose, among other compounds of composted urban waste that barely appeared in pyrolytic liquids.

Compounds	Formula	MS	RT (min)	Area (%)
<i>2-methylpropan-1-ol</i>	$C_4H_{10}O$	74.12	4.140	5.27
<i>1-pentanol</i>	$C_5H_{12}O$	88.15	4.255	4.69
<i>pent-1-en-3-yne</i>	C_5H_6	66.10	4.320	2.93
<i>2-methylpropanal</i>	C_4H_8O	72.11	4.425	3.40
<i>hexanal</i>	$C_6H_{11}O$	100.16	4.660	5.04
<i>2,2-dimethylpropanenitrile</i>	C_5H_9N	83.13	4.965	3.37
<i>(3E)-hexa-1,3,5-triene</i>	C_6H_8	80.13	5.195	5.25
<i>4-methylpenta-1,3-diene</i>	C_6H_{10}	82.14	5.315	3.60
<i>hexa-1,5-diyne</i>	C_6H_6	78.11	5.470	3.82
<i>(3E)-hexa-3,5-dien-2-ol</i>	$C_6H_{10}O$	98.14	5.565	4.04
<i>2,2-dimethylpropanal</i>	$C_5H_{10}O$	86.13	5.935	5.48
<i>2-methylpent-4-en-1-ol</i>	$C_6H_{12}O$	100.16	5.990	2.60
<i>2,5-dimethylfuran</i>	C_6H_8O	96.13	6.130	4.45

<i>(5E)-hepta-1,5-diene</i>	C ₇ H ₁₂	96.17	6.510	3.75
<i>ethenyl acetate</i>	C ₄ H ₆ O ₂	86.09	6.665	4.80
<i>5-methylhexa-1,4-diene</i>	C ₇ H ₁₂	96,17	6.985	5.18
<i>(3E)-2-methylhexa-1,3,5-triene</i>	C ₇ H ₁₀	94.15	7.115	4.64
<i>3-prop-2-enylcyclopentene</i>	C ₈ H ₁₂	108.18	7.270	5.25
<i>(5E)-hepta-1,5-dien-3-yne</i>	C ₇ H ₈	92.14	7.755	4.98
<i>cyclopentanone</i>	C ₅ H ₈ O	84.12	8.340	4.35
<i>octane</i>	C ₈ H ₁₈	114.23	8.595	3.59
<i>methyl 2-methylpropyl carbonate</i>	C ₆ H ₁₂ O ₃	132.16	10.545	2.75
<i>1,3-xylene</i>	C ₈ H ₁₀	106.16	10.715	3.29
<i>1,2-xylene</i>	C ₈ H ₁₀	106.16	10.965	3.47

Table 5. Main compounds found by GC/MS in non-condensable gases of MSW compost pyrolysis at 450°C.

A significant amount of alcohols (16.6%) is found in organic gases, such as 2-methylpropan-1-ol (5.3%), 1-pentanol (4.7%), (3E)-hexa-3,5-dien-2-ol (4.0%) or 2-methylpent-4-en-1-ol (2.6%). There is also a wide variety of aldehydes (13.9%) such as 2-methylpropanal (3.4%), hexanal (5.0%) or 2,2-dimethylpropanal (5.5%). Some compounds derived from hemicellulose and cellulose are also observed, mainly 2,5-dimethylfuran (4.5%). The same compound was also found by Hubble and Goldfarb (2021) in hemicelluloses pyrolytic degradation. A group of compounds derived from plastics and other compounds of more specific urban solid waste can be distinguished, as in the case of 1,3-xylene and 1,2-xylene (3.3% and 3.5%, respectively).

It should be noted that numerous organic compounds with double and triple bonds (36.6%) are obtained from the degradation of carbohydrates, proteins and other typical components of organic matter of animal or human origin (Somorin et al., 2020). The compost has been produced from solid urban waste from

1
2
3 coastal area and is made up of various remains of seashells and bones, so these
4
5 chemical compounds from its decomposition are common.
6

7 8 **4. Conclusions** 9

10 The behaviour of MSW compost and products formed in fluidized bed pilot plant
11 is similar to that established on lignocellulosics raw material. Four characteristic
12 zones (humidity evolution, hemicellulose decomposition, lignin and cellulose
13 degradation and lignin disintegration) have been found.
14
15
16
17

18 The TGA evolution and its kinetic constants similar to those found for
19 lignocellulosic materials have been measured. However, the produced biochar
20 has low stability and aromaticity due to its high and low O/C and H/C ratios,
21 respectively. Additionally, the compounds found in the bio-oil as highly phenolics
22 can be described, it could be due to its humic and fulvic compounds (heavy
23 compounds) in the original material (compost) as well as lignin not degraded
24 during the composting process. Moreover, the compounds in non-condensable
25 gases to thermal degradation of shorter structures such as hemicellulose,
26 proteins and cellulose may be due.
27
28
29
30
31
32
33
34
35
36
37
38
39

40 **Acknowledgments** 41

42 This project (PID2020-112875RB-C21) has been supported by the State
43 Research Agency (SRA - Spanish Ministry of Economy and Competitiveness
44 through the National Programme for Research Aimed at the Challenges of
45 Society) and European Regional Development Fund (ERDF), the Regional
46 Ministry of Innovation, Science and Enterprise, Government of the Junta de
47 Andalucía (Operational Programme FEDER Andalusia 2014-2020. Project UHU-
48 1255540) and research and knowledge transfer micro-projects "Cátedra de la
49
50
51
52
53
54
55
56
57
58
59
60

1
2
3 Provincia", University of Huelva, Spain. Funding for the open access fee is
4
5 provided by the University of Huelva / CBUA.
6
7

8 **5. References**

9
10 Açıklın K and Gözke, G (2021) Thermogravimetric pyrolysis of onion skins:
11
12 Determination of kinetic and thermodynamic parameters for devolatilization
13
14 stages using the combinations of isoconversional and master plot methods.
15

16 *Bioresource Technology* 342: 125936.
17

18
19 Agirre I, Griessacher T, Rösler G, et al. (2013) Production of charcoal as an
20
21 alternative reducing agent from agricultural residues using a semi-
22
23 continuous semi-pilot scale pyrolysis screw reactor. *Fuel Processing*
24
25 *Technology* 106: 114-121.
26

27
28 Ahmad M, Lee SS, Dou X, et al. (2012) Effects of pyrolysis temperature on
29
30 soybean stover- and peanut shell-derived biochar properties and TCE
31
32 adsorption in water. *Bioresource Technology* 118: 536-544.
33

34
35 Ansah E, Wang L and Shahbazi A (2016) Thermogravimetric and calorimetric
36
37 characteristics during co-pyrolysis of municipal solid waste components.
38
39 *Waste Management* 56: 196-206.
40

41
42 Ansari KB, Arora JS, Chew JW, et al. (2018) Effect of Temperature and Transport
43
44 on the Yield and Composition of Pyrolysis-Derived Bio-Oil from Glucose.
45
46 *Energy Fuels* 32(5): 6008-6021.
47

48
49 Baigorri R, Fuentes M, González-Gaitano G, et al. (2009) Complementary
50
51 multianalytical approach to study the distinctive structural features of the
52
53 main humic fractions in solution: Gray humic acid, brown humic acid, and
54
55 fulvic acid. *Journal of Agricultural and Food Chemistry* 57: 3266-3272.
56

57
58 Beis SH, Onay Ö, Koçkar ÖM (2002) Fixed-bed pyrolysis of safflower seed:
59
60

1
2
3 Influence of pyrolysis parameters on product yields and compositions.
4
5 *Renewable Energy* 26(1): 21-32.
6

7 Boateng AA, Mullen CA, Osgood-Jacobs L, et al. (2012) Mass Balance, Energy,
8 and Exergy Analysis of Bio-Oil Production by Fast Pyrolysis. *Journal of*
9
10 *Energy Resources Technology* 134(4): 042001.
11
12

13
14 Buah WK, Cunliffe AM and Williams PT (2007) Characterization of Products from
15 the Pyrolysis of Municipal Solid Waste. *Process Safety and Environmental*
16
17 *Protection* 85(5): 450-457.
18
19

20
21 Collard FX and Blin J (2014) A review on pyrolysis of biomass constituents:
22 Mechanisms and composition of the products obtained from the conversion
23 of cellulose, hemicelluloses and lignin. *Renewable and Sustainable Energy*
24
25 *Reviews* 38: 594-608.
26
27

28
29 Dang H, Wang G, Wang C, et al. (2021) Comprehensive Study on the Feasibility
30 of Pyrolysis Biomass Char Applied to Blast Furnace Injection and Tuyere
31
32 Simulation Combustion. *ACS Omega* 6(31): 20166-20180.
33
34

35
36 Delgado-Rodríguez M, Ruiz-Montoya M, Giraldez I, et al. (2011) Influence of
37 control parameters in VOCs evolution during MSW trimming residues
38
39 composting. *Journal of Agricultural and Food Chemistry* 59(24): 13035-
40
41 13042.
42
43

44
45 Dhyani V, Kumar M, Wang Q, et al. (2018) Effect of composting on the thermal
46 decomposition behavior and kinetic parameters of pig manure-derived solid
47
48 waste. *Bioresource Technology* 252: 59-65.
49
50

51
52 Di Blasi C, Gonzalez Hernandez E and Santoro A (2000) Radiative Pyrolysis of
53 Single Moist Wood Particles. *Industrial & Engineering Chemistry Research*
54
55 39(4): 873-882.
56
57
58
59
60

- 1
2
3 Díaz MJ, Ruiz-Montoya M, Palma A, et al. (2021) Thermogravimetry applicability
4 in compost and composting research: A review. *Applied Sciences* 11(4): 1-
5 15.
6
7
8
9
10 EEA (2020) Bio-waste in Europe-turning challenges into opportunities. European
11 Environment Agency, Report No 04/2020, Denmark.
12
13
14 El-Sayed SA and Mostafa ME (2015) Kinetic Parameters Determination of
15 Biomass Pyrolysis Fuels Using TGA and DTA Techniques. *Waste and*
16 *Biomass Valorization* 6: 401-415.
17
18
19
20
21 Fabbri D, Torri C and Spokas KA (2012) Analytical pyrolysis of synthetic chars
22 derived from biomass with potential agronomic application (biochar).
23 Relationships with impacts on microbial carbon dioxide production. *Journal*
24 *of Analytical and Applied Pyrolysis* 93: 77-84.
25
26
27
28
29
30 Fachini J, Figueiredo CC, Frazão JJ, et al. (2021) Novel K-enriched
31 organomineral fertilizer from sewage sludge-biochar: Chemical, physical and
32 mineralogical characterization. *Waste Management* 135: 98-108.
33
34
35
36
37
38 Fernández-López M, Pedrosa-Castro GJ, Valverde JL, et al. (2016) Kinetic
39 analysis of manure pyrolysis and combustion processes. *Waste*
40 *Management* 58: 230-240.
41
42
43
44
45 Ferreira OC (2000) Emissions of greenhouse gases in the production and use of
46 plant charcoal. *Revista Economia & Energia* 1: 1-16.
47
48
49 Fidel RB, Laird DA, Thompson ML, et al. (2017) Characterization and
50 quantification of biochar alkalinity. *Chemosphere* 167: 367-373.
51
52
53
54 Finney KN, Ryu C, Sharifi VN, et al. (2009) The reuse of spent mushroom
55 compost and coal tailings for energy recovery: Comparison of thermal
56 treatment technologies. *Bioresource Technology* 100(1): 310-315.
57
58
59
60

- 1
2
3 Flynn JH and Wall LA (1966). General treatment of the thermogravimetry of
4 polymers. *Journal of Research of the National Bureau of Standards - A.*
5
6 *Physics and Chemistry* 70A(6): 487-523.
7
8
9
10 Garrido R, Ruiz-Felix MN and Satrio JA (2012) Effects of Hydrolysis and
11
12 Torrefaction on Pyrolysis Product Distribution of Spent Mushroom Compost
13
14 (SMC). *International Journal of Environmental Pollution and Remediation* 1:
15
16 98-103.
17
18
19 Ghodake GS, Shinde SK, Kadam AA, et al. (2021) Review on biomass
20
21 feedstocks, pyrolysis mechanism and physicochemical properties of biochar:
22
23 State-of-the-art framework to speed up vision of circular bioeconomy.
24
25 *Journal of Cleaner Production* 297: 126645.
26
27
28 Ghorbel L, Rouissi T, Brar SK, et al. (2015) Value-added performance of
29
30 processed cardboard and farm breeding compost by pyrolysis. *Waste*
31
32 *Management* 38: 164-173.
33
34
35 Giwa AS, Xu H, Wu J, et al. (2018) Sustainable recycling of residues from the
36
37 food waste (FW) composting plant via pyrolysis: Thermal characterization
38
39 and kinetic studies. *Journal of Cleaner Production* 180: 43-49.
40
41
42 Guizani C, Haddad K, Limousy L, et al. (2017) New insights on the structural
43
44 evolution of biomass char upon pyrolysis as revealed by the Raman
45
46 spectroscopy and elemental analysis. *Carbon* 119: 519-521.
47
48
49 Gunasee SD, Carrier M, Gorgens JF, et al. (2016) Pyrolysis and combustion of
50
51 municipal solid wastes: Evaluation of synergistic effects using TGA-MS.
52
53 *Journal of Analytical and Applied Pyrolysis* 121: 50-61.
54
55
56 Hameed M, Bhat RA, Pandit BA, et al. (2021) Qualitative assessment of compost
57
58 engendered from municipal solid waste and green waste by indexing
59
60

1
2
3 method. *Journal of the Air & Waste Management Association* 72(2): 210-
4
5 219.

6
7 Huang YF, Kuan WH, Chiueh PT, et al. (2011) Pyrolysis of biomass by thermal
8
9 analysis-mass spectrometry (TA-MS). *Bioresource Technology* 102(3):
10
11 3527-3534.

12
13 Hubble AH and Goldfarb JL (2021) Synergistic effects of biomass building blocks
14
15 on pyrolysis gas and bio-oil formation. *Journal of Analytical and Applied*
16
17 *Pyrolysis* 156: 105100.

18
19 Jaroenkhasemmesuk C and Tippayawong N (2015) Technical and Economic
20
21 Analysis of A Biomass Pyrolysis Plant. *Energy Procedia* 79: 950-955.

22
23 Jiang KM, Cheng CG, Ran M, Lu YG (2018) Preparation of a biochar with a high
24
25 calorific value from chestnut shells. *New Carbon Materials* 33(2): 183-187.

26
27 Joyce JF, Sato C, Cardenas R (1998) Composting of polycyclic aromatic
28
29 hydrocarbons in simulated municipal solid waste. *Water Environment*
30
31 *Research* 70(3): 356-361.

32
33 Kebelmann K, Hornung A, Karsten U (2013) Intermediate pyrolysis and product
34
35 identification by TGA and Py-GC/MS of green microalgae and their extracted
36
37 protein and lipid components. *Biomass and Bioenergy* 49: 38-48.

38
39 Kim KH, Kim TS, Lee SM, et al. (2013) Comparison of physicochemical features
40
41 of biooils and biochars produced from various woody biomasses by fast
42
43 pyrolysis. *Renewable Energy* 50: 188-195.

44
45 Larina OM and Zaichenko VM (2018) Thermal cracking in charcoal and ceramics
46
47 of pyrolysis liquid from sewage sludge. *Journal of Physics: Conference*
48
49 *Series* 946: 012034.

50
51 Li M, Liu Q, Guo L, et al. (2013) Cu(II) removal from aqueous solution by *Spartina*
52
53
54
55
56
57
58
59
60

- 1
2
3 alterniflora derived biochar. *Bioresource Technology* 141: 83-88.
4
5 Mierzwa-Hersztek M, Gondek K, Jewiarz M, et al. (2019) Assessment of energy
6 parameters of biomass and biochars, leachability of heavy metals and
7 phytotoxicity of their ashes. *Journal of Material Cycles and Waste*
8 *Management* 21: 786-800.
9
10
11
12
13
14 Mohan D, Pittman CU and Steele PH (2006) Pyrolysis of Wood/Biomass for Bio-
15 oil: A Critical Review. *Energy Fuels* 20(3): 848-889.
16
17
18
19 Morin M, Pécate S, Hémati M, et al. (2016) Pyrolysis of biomass in a batch
20 fluidized bed reactor: Effect of the pyrolysis conditions and the nature of the
21 biomass on the physicochemical properties and the reactivity of char. *Journal*
22 *of Analytical and Applied Pyrolysis* 122: 511-523.
23
24
25
26
27
28 Ozawa T (1965) A New Method of Analyzing Thermogravimetric Data. *Bulletin of*
29 *the Chemical Society of Japan* 38(11): 1881-1886.
30
31
32
33
34
35
36
37
38
39
40
41
42
43
44
45
46
47
48
49
50
51
52
53
54
55
56
57
58
59
60
- Palma A, Doña-Grimaldi VM, Ruiz-Montoya M, et al. (2020) MSW compost valorization by pyrolysis: Influence of composting process parameters. *ACS Omega* 5(33): 20810-20816.
- Parthasarathy P, Al-Ansari T, Mackey HR, et al. (2021) Effect of heating rate on the pyrolysis of camel manure. *Biomass Conversion Biorefinery* 13: 6023-6035.
- Pietro M and Paola C (2004) Thermal analysis for the evaluation of the organic matter evolution during municipal solid waste aerobic composting process. *Thermochimica Acta* 413 (1-2): 209-214.
- Qian Q, Machida M and Tatsumoto H (2007) Preparation of activated carbons from cattle-manure compost by zinc chloride activation. *Bioresource Technology* 98(2): 353-360.

- 1
2
3 Rangabhashiyam S and Balasubramanian P (2019) The potential of
4 lignocellulosic biomass precursors for biochar production: Performance,
5 mechanism and wastewater application—A review. *Industrial Crops and*
6 *Products* 128: 405-423.
7
8
9
10
11
12 Rashid MI and Shahzad K (2021) Food waste recycling for compost production
13 and its economic and environmental assessment as circular economy
14 indicators of solid waste management. *Journal of Cleaner Production* 317:
15 128467.
16
17
18
19
20
21 Sánchez-Silva L, Gutiérrez N, Romero A, et al. (2012) Pyrolysis and combustion
22 kinetics of microcapsules containing carbon nanofibers by thermal analysis-
23 mass spectrometry. *Journal of Analytical and Applied Pyrolysis* 94: 246-252.
24
25
26
27
28 Shakya A and Agarwal T (2017) Poultry Litter Biochar: An Approach towards
29 Poultry Litter Management - A Review. *International Journal of Current*
30 *Microbiology and Applied Sciences* 6(10): 2657-2668.
31
32
33
34
35 Soh M, Chew JJ, Liu S, et al. (2019) Comprehensive Kinetic Study on the
36 Pyrolysis and Combustion Behaviours of Five Oil Palm Biomass by
37 Thermogravimetric-Mass Spectrometry (TG-MS) Analyses. *Bioenergy*
38 *Research* 12: 370-387.
39
40
41
42
43
44 Somorin T, Parker A, McAdam E, et al. (2020) Pyrolysis characteristics and
45 kinetics of human faeces, simulant faeces and wood biomass by
46 thermogravimetry-gas chromatography-mass spectrometry methods.
47 *Energy Reports* 6: 3230-3239.
48
49
50
51
52
53 Soobhany N, Gunasee S, Rago YP, et al. (2017) Spectroscopic,
54 thermogravimetric and structural characterization analyses for comparing
55 Municipal Solid Waste composts and vermicomposts stability and maturity.
56
57
58
59
60

1
2
3 *Bioresource Technology* 236: 11-19.
4

5 Tagade A, Kirti N and Sawarkar AN (2021) Pyrolysis of agricultural crop residues:
6 An overview of researches by Indian scientific community. *Bioresource*
7 *Technology Reports* 15: 100761.
8
9

10
11
12 Tripathi M, Sahu JN and Ganesan P (2016) Effect of process parameters on
13 production of biochar from biomass waste through pyrolysis: A review.
14
15
16
17 *Renewable and Sustainable Energy Reviews* 55: 467-481.
18

19 Tsai CH, Tsai WT, Liu SC, et al. (2018) Thermochemical characterization of
20 biochar from cocoa pod husk prepared at low pyrolysis temperature.
21
22
23
24 *Biomass Conversion and Biorefinery* 8: 237-243.
25

26 Wei L, Huang Y, Huang L, et al. (2020) The ratio of H/C is a useful parameter to
27 predict adsorption of the herbicide metolachlor to biochars. *Environmental*
28
29
30
31 *Research* 184: 109324.
32

33 Xiao X, Chen Z and Chen B (2016) H/C atomic ratio as a smart linkage between
34
35
36
37
38
39
40
41
42
43
44
45
46
47
48
49
50
51
52
53
54
55
56
57
58
59
60
pyrolytic temperatures, aromatic clusters and sorption properties of biochars
derived from diverse precursory materials. *Scientific Reports* 6: 22644.

Xie K, Hu H, Cao J, et al. (2020) A novel method for salts removal from municipal
solid waste incineration fly ash through the molten salt thermal treatment.
Chemosphere 241: 125107.

Pyrolysis of Municipal Solid Waste compost: pilot plant evaluation as a sustainable practise of waste management

A. Palma ^{*,a}, S. Clemente-Castro ^a, M. Ruiz-Montoya ^a, I. Giráldez ^b, M.J. Díaz ^a

Pro²TecS–Product Technology and Chemical Processes Research Centre

^aDepartment of Chemical Engineering, Physical Chemistry and Materials Science

^bDepartment of Chemistry “Prof. José Carlos Vilchez Martín”

University of Huelva. Campus “El Carmen”, 21071, Huelva (Spain)

*Corresponding author: alberto.palma@diq.uhu.es

Abstract

To evaluate the potential of compost based on Municipal Solid Waste (MSW) and 20% legume pruning under a pyrolysis process, generated products, including solids (biochar), liquids (bio-oil) and gases (non-condensable gases), through experimentation in a pilot plant with a fluidised bed reactor at 450 °C and gas chromatography/mass spectrometry (GC/MS) have been analysed. Also, the compost kinetic behaviour by thermogravimetric analysis (TGA), using Flynn-Wall-Ozawa method, has been investigated. Four different reaction zones, associated with lignocellulosic materials (hemicellulose, cellulose and lignin) with a first step for water evaporation, in TGA curve have been observed. A biochar with low stability and aromaticity, considering high and low O/C and H/C ratios, respectively, has been obtained. The obtained pyrolytic liquids contain a high concentration of phenolic compounds because of a significant presence of lignins and other high molecular weight compounds in the original material. Moreover, the generated non-condensable gases consist mainly of short-chain compounds such as alcohols, aldehydes and alkenes produced from hemicellulose, cellulose and proteins.

Keywords: pyrolysis; MSW compost; kinetic; GC/MS; biochar.

1. Introduction

It has been widely recognised that inadequate treatment of organic waste can lead to significant environmental and health problems. In this respect, the beneficial properties of compost both as a suitable solution for the treatment and sanitation of organic waste and its subsequent use in agriculture (both technically and economically) have been extensively demonstrated (Rashid and Shahzad, 2021). Despite the problems that inadequate management, mainly due to the odours emitted (Delgado-Rodríguez et al., 2011) can cause.

The quality of the final compost will depend significantly on the nature and quality of the waste to be composted. However, the process parameters are also involved in the degradation to which the organic compounds are subjected during composting. Therefore, a high variability of quality in the produced compost can be ascertained, and quality standards for its use in agriculture must be applied (Hameed et al., 2021). However, in addition to the traditional uses of compost, new uses and organo-mineral formulations (Fachini et al., 2021) are being developed.

In the EU-28 (28 EU Member States) approximately 88 million tonnes/year of food are wasted. About 20% of the food produced represents this value. Because of various problems, including lack of segregated sorting and impurities, only 17% of this municipal waste can be properly composted and/or digested (EEA, 2020). Therefore, a high proportion of composted Municipal Solid Waste (MSW) is not of a quality suitable for direct use in agriculture.

Consequently, various ways of valorization of this compost of low agronomic quality, apart from the alternative uses that are already being used, such as the recovery of degraded areas (mines, quarries, landfills), forestry crops, etc.,

1
2
3 should be explored. Therefore, enhancing the valorisation pathways of these
4 materials to improve the management of these wastes should be developed.
5

6
7 Thermochemical processes, due to the wide range of products (solid, liquid and
8 gaseous) and/or energy generated, are an alternative to be considered for the
9 valorisation of organic materials. Among these, combustion (with an excess of
10 oxygen over that required according to stoichiometry), gasification (with a deficit
11 of oxygen over that required according to stoichiometry) and pyrolysis (without
12 oxygen) can be noted (Beis et al., 2002).
13
14
15
16
17
18
19
20

21 In this sense, pyrolytic processes as a source of new high value-added products
22 from compost can be highlighted. During composting, organic compounds are
23 generally degraded or directly mineralized, although a portion of the high
24 molecular weight compounds present in the original material increase the degree
25 of aromaticity in the resulting composted compounds. Also, an increase in the
26 mass degradation above 600 °C as the composting time increases (Díaz et al.,
27 2021) is produced. Thus, the composting process significantly alters the
28 distribution of chemical compounds and may result in products that may not be
29 produced during pyrolysis of other sources of organic compounds.
30
31
32
33
34
35
36
37
38
39
40
41

42 Among these innovative materials from compost by pyrolysis, Qian et al. (2007)
43 and Finney et al. (2009) used compost, from livestock manure and mushroom
44 industry residues, respectively, as raw material for the production of biochar.
45 Also, the use of composts, in the pyrolysis process, as a potential feedstocks for
46 bio-oil production has been studied by Garrido et al. (2012) and Giwa et al.
47 (2018).
48
49
50
51
52
53
54

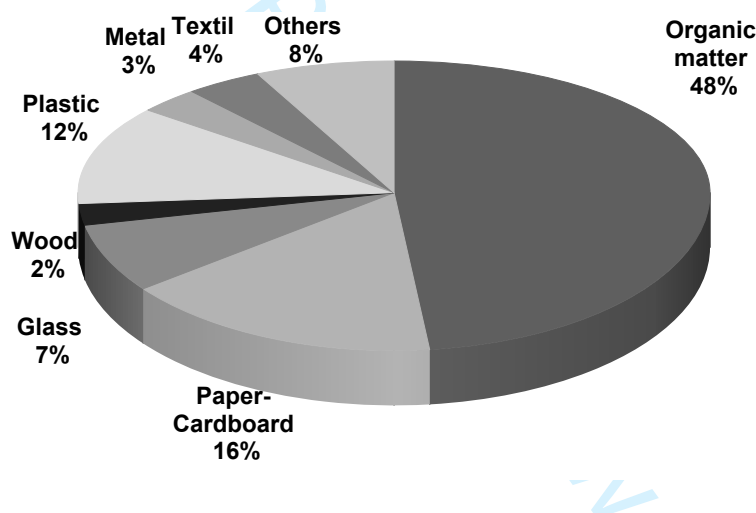
55 The general objective of this work is to study the products generated (biochar,
56 pyrolytic liquids and volatile organic compounds) during the pyrolysis of MSW
57
58
59
60

1
2
3 compost with 20% pruning residues. Also, the kinetics of the reactions produced
4
5 during the pyrolysis of these composts has been studied.
6
7

8 **2. Materials and Methods**

9 **2.1. MSW composition**

10
11 The different components of MSW can be classified into three main groups:
12 fermentable (food waste), combustible (paper, cardboard, plastics, rubber,
13
14
15
16
17
18
19
20
21
22
23
24
25
26
27
28
29
30
31
32
33
34
35
36
37
38
39
40
41
42
43
44
45
46
47
48
49
50
51
52
53
54
55
56
57
58
59
60
The composition of MSW is highly variable and depends on factors such as the standard of living, lifestyle of the population, and the time of year. The composition of the MSW composted in this study is shown in Figure 1.



41
42
43
44
45
46
47
48
49
50
51
52
53
54
55
56
57
58
59
60
Figure 1. MSW composition.

46 **2.2. Compost characteristics**

49
50
51
52
53
54
55
56
57
58
59
60
Non-selective Municipal Solid Waste Compost (MSWC) from Villarrasa (Huelva - Spain) urban waste treatment plant is used in this study. Prior to composting the main treatment involves trammel-screening (8 cm), metal electromagnetic separation and manual separation of plastics. To improve internal aeration in composting piles, 20% of bulking material (legume pruning of *Leucaena*

leucocephala), before the composting process, have been added. The non-degraded fraction of this material was separated by screening at the end of the composting process. The most relevant chemical characteristics of the final compost are reported in Table 1.

Property	Units	Compost (after 40 days)
pH (1:5 extract)		7.8 ± 1.2
EC (1:5 extract)	dS m ⁻¹	8.5 ± 1.1
Organic Matter	g kg ⁻¹	593 ± 32
Kjeldahl-N	g kg ⁻¹	12.3 ± 3.5
Ash	g kg ⁻¹	35.4 ± 4.7
C/N		26.6
Moisture	%	0.6

^a Determined in MSW <5 mm and free of impurities

^b Mean values and standard deviations were calculated from the triplicates

Table 1. Relevant characteristics of used MSWC^a (average ± standard deviation)^b

2.3. Processing of the samples by pyrolysis with TGA

The dried compost samples, with an initial average diameter of 50 mm, were milled into particles of smaller size (1-2 mm). The final particles were stored without contact with air moisture. Thermochemical decomposition behavior was evaluated using a thermo-gravimetric analyzer (TGA) (Mettler Toledo TGA/DSC1 STARe System). TGA experiments heating 10-25 mg samples from 25 °C to 850 °C, at four heating rates (5, 10, 15 and 20 °C min⁻¹) under nitrogen flow rate of 20 cm³ min⁻¹ have been performed. The obtained thermo-gravimetric analysis data

1
2
3 for any changes in the thermo-chemical decomposition behavior have been
4
5 studied.

6 7 8 **2.4. Pilot plant pyrolysis**

9
10 A laboratory-scale fluidized bed reactor (PID Eng&Tech Micromeritics) has been
11
12 employed. An operating temperature of 450 °C has been used. 30 L min⁻¹ of
13
14 nitrogen (twice the minimum fluidization rate) has been used, with a constant
15
16 pressure difference of 33 mbar.

17
18 A gas cleaning system at the reactor outlet has been installed. This system
19
20 consists of two cyclones (CY1 for particles >20µm and CY2 for particles >5µm)
21
22 that have been connected in series. Downstream, a heat exchanger (400°C to
23
24 90°C), controlled by a single valve, is used to regulate the inflow of the coolant
25
26 fluid (water 20°C) into the heat exchanger. Pyrolytic liquids in a cooling vessel
27
28 (first condenser (CD1) at 63 °C), located at the bottom of the heat exchanger
29
30 have been collected. Water and other condensed liquids are retained in a second
31
32 condenser (CD2) (30°C). Finally, the product gases pass through coalescing
33
34 filters before sampling and finally into a scrubber (23°C).

35 36 37 38 39 **2.5. Pyrolytic liquid analysis**

40
41 An aliquot to pyrolytic liquid has been extracted with water (1:10 ratio), vortexed
42
43 30 s and centrifugation for 20 min at 5000 rpm. Then, 1 mL the water-insoluble
44
45 fraction was extracted with diethyl ether (DEE) (3 x 1 mL). After extraction, an
46
47 aliquot DEE extract (500 µL) has been dried under nitrogen and 50 µL of both
48
49 pyridine and BSTFA/TMCS (90:10) were added following incubated for 30 min at
50
51 60°C. Then, TMS derivative extracts were diluted (1:10) with CHCl₃ and 1 µL was
52
53 injected into GC-MS/MS (GCMSQP8030 Ultra System, Shimadzu, Japan). TMS
54
55 derivative compounds were separated by a HP-5 MS column (60 m, 0.25 mm I.D.).
56
57
58
59
60

0.25 μm film thickness, J&W Scientific, Agilent Technologies, USA). The GC oven was programmed: 50 $^{\circ}\text{C}$ for 2 min, ramped at 8 $^{\circ}\text{C min}^{-1}$ to 280 $^{\circ}\text{C}$, held for 2 min. A second ramp rate was performed of 50 $^{\circ}\text{C min}^{-1}$ until a final temperature of 300 $^{\circ}\text{C}$ was reached and held for 2 min. Helium at constant flow rate of 1.20 mL min^{-1} was used as the carrier gas. The temperatures of the injection port (split mode 10:1), transfer line and ion source were maintained at 250, 280 and 230 $^{\circ}\text{C}$, respectively. The mass spectrometer was operated in scan mode (50-800 m z^{-1}). TMS derivative compounds were identified by comparison of the mass spectra with those of the database of NIST11 library. For control and data analysis, GCMS Postrun Analysis Shimadzu was used. The MS was turned with perfluorotributylamine (PFTBA).

2.6. Biochar analysis

Gross Calorific Value (constant volume) following the standards "CEN/TS 14918:2005 (E) Solid Biofuels - Method for the determination of the calorific value" and UNE 164001 EX have been determined. Automatic Isoperibol Calorimeter Parr 6300 has been used. Total carbon, hydrogen and sulphur simultaneously in a ELTRA Carbon/Hydrogen/Sulfur Analyzer CHS-580A (ELTRA GmbH, Germany) have been determined. The standard guidelines for the determination of carbon, hydrogen (EN 15104:2011) and sulfur (EN 15289:2011) have been followed. Moreover, oxygen content by difference (CEN/TS 14961, 2005) has been also calculated. According to ISO 10390:2005, biochar was air-dried and crushed into fine particles (<2 mm). Then, the sample was soaked with 0.01 M CaCl_2 at a 1:5 solid/water ratio for 1 h with agitation.

1
2
3 After still standing for 1 h, the slurry was then measured for pH using a pH-meter
4 GLP 21 (Crison Instruments, S.A.).
5
6

7 **2.7. Volatile compounds gas samples analysis by pyrolysis TD/GC-MS**

8
9
10 Volatile compounds gas samples from the pilot plant pyrolysis process at 350 and
11 550°C (corresponding to higher temperatures than the degradation maxima found
12 in the TGA curves) were collected in fritted glass TD tubes (Supelco, Bellefonte,
13 PA; O.D.: 6.35 mm; length: 88.9 mm) for 1.5 min. Tubes containing 100 mg of
14 Tenax® TA (80-100 mesh purchased from Supelco, Bellefonte, PA) packed in
15 layers of silanized glass wool. TD tubes after sampling have been analyzed using
16 TD/GC-MS. TD was used to release the captured volatile compounds from the
17 tube sorbent material onto the GC/MS for identification and quantification. TD
18 was carried out by use of thermal desorption system unit (TD-20, Shimadzu,
19 Japan) fitted with a HP-5 MS column (60 m, 0.25 mm I.D. 0.25 µm film thickness,
20 J&W Scientific, Agilent Technologies, USA) and involved 2 steps: tube desorption
21 and trap desorption. The mass spectrometer was operated in scan mode (41-450
22 m z⁻¹). Volatile organic compounds were identified by comparison of the mass
23 spectra with those of in the database of NIST11 library using as internal standard
24 1-bromo-3-chlorobenzene (BCB). For control and data analysis, the GCMS
25 Postrun Analysis Shimadzu was used. The MS was turned with
26 perfluorotributylamine (PFTBA).
27
28
29
30
31
32
33
34
35
36
37
38
39
40
41
42
43
44
45
46
47
48

49 **2.8. Kinetic analysis by Flynn-Wall-Ozawa method**

50
51 The activation energy of pyrolysis reactions in lignocellulosic materials has been
52 studied by several different mathematical methods. In this regard, the use of
53 isoconversional methods for the determination of pyrolysis kinetics has been
54 successfully documented (Açıklalın and Gözke, 2021). Moreover, according to the
55
56
57
58
59
60

1
2
3 results obtained by Fernández-López et al. (2016) and Palma et al. (2020), this
4 model has been satisfactorily tested in different composts. Moreover, Gunasee
5 et al. (2016) have demonstrated that this TGA-based experimental methodology
6 could be suitable for revealing synergistic reactions during co-pyrolysis of
7 different MSW.
8
9

10 For a given reaction, the activation energy should be a constant value throughout
11 the weight loss region, so changes in these values imply degradation of other
12 compounds. In the present study the activation energy values for the degradation
13 process using the Flynn-Wall-Ozawa (FWO) isoconversional method (Flynn and
14 Wall, 1966; Ozawa, 1965) defined by Eq. 1 have been determined. This method
15 for determination of the E_a values without any knowledge of its mechanisms (El-
16 Sayed and Mostafa, 2015) can be used.
17
18
19
20
21
22
23
24
25
26
27
28
29

$$30 \ln(\beta) = \ln\left(\frac{A E_a}{R g(\alpha)}\right) - 2.315 - 0.4567 \frac{E_a}{RT} \quad (\text{Eq. 1})$$

31 where β is the heating rate, A is the pre-exponential factor, $g(\alpha)$ is a function of
32 the conversion, E_a is the activation energy and R is the gas constant.
33
34
35
36
37

38 Therefore, for different heating rates (β) and a given degree of conversion (α), a
39 linear relationship is observed by plotting of natural logarithm of heating rates (\ln
40 β), versus $(1/T)$ obtained from thermal curves recorded at different heating rates
41 will be a straight line whose slope $(-0.4567 (E_a/RT))$ will calculate the activation
42 energy.
43
44
45
46
47
48
49

50 **3. Result and Discussion**

51 **3.1. Compost TGA analysis**

52 Thermograms of compost (TGA) and their derivative (DTG) with respect to
53 temperature corresponding to pyrolytic decomposition of MSWC, at $20^\circ\text{C min}^{-1}$
54
55
56
57
58
59
60

are shown in Figure 2 (for the kinetic parameters calculation four thermograms, at four heating rates 5, 10, 15 and 20°C min⁻¹, have been carried out. To show the evolution only the last thermogram has been displayed. In this form, the mass loss profile (TGA) and its derivative curve (DTG) obtained by thermogravimetric analysis are shown in Figure 2.

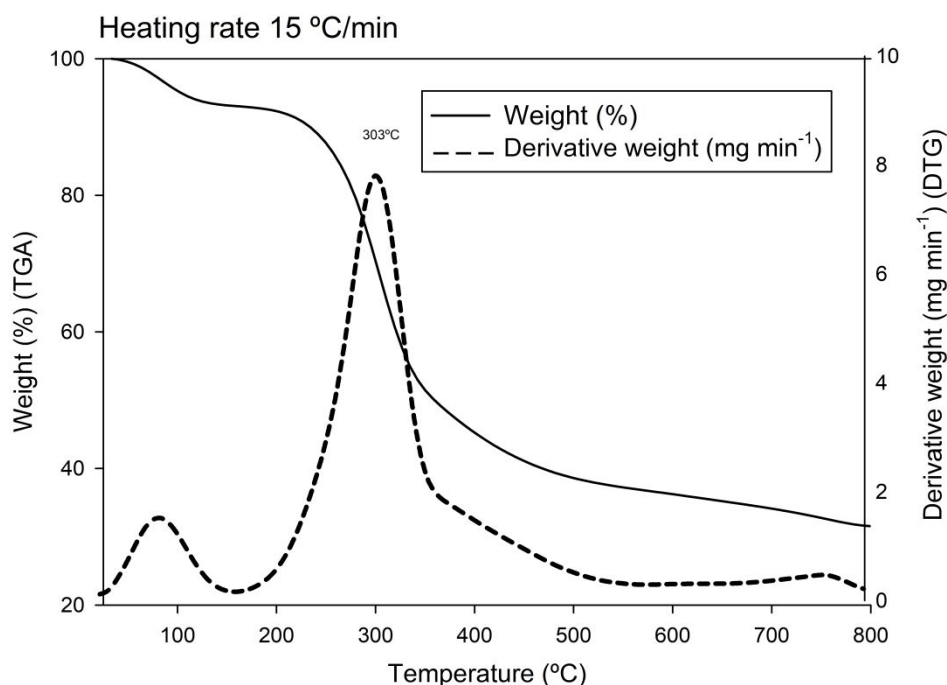


Figure 2. TGA and DTG correspond to MSW Compost pyrolytic degradation at 20°C min⁻¹.

The figure shows the typical evolution described by different researchers (Dhyani et al., 2018). Similar to what was observed by López-González et al. (2014) in the pyrolysis process of manure compost, a thermochemical behavior similar to that of lignocellulosic biomass can be observed. In this evolution the three main phases in the thermal degradation of compost: phase I between 25 and 120 °C; phase II between 200 °C and 400 °C and phase III between 400 °C and 700 °C can be observed. The peak found (DTG) in the first phase (<200°C) corresponds

1
2
3 to the dehydration process of the compost sample although some authors
4 indicate that decarboxylation may also occur in labile compounds (Pietro and
5 Paola, 2004). The main peak (DTG) in the second phase (200-350 °C) can be
6 identified and a weight loss over 44% at this stage can be calculated. This second
7 peak to the thermal degradation of simple organic matter and semi-volatile
8 compounds such as hemicelluloses, cellulose, degradation of aliphatic structures
9 and microbial cell walls can be associated (Baigorri et al., 2009). The data
10 reported in this study are similar to those presented by Sánchez-Silva et al.
11 (2012) for which a significant weight loss between 210 and 373 °C has been
12 reported. This implies a lower temperature range than that found for the different
13 lignocellulosic biomasses, which are usually between 200 and 450 °C. This fact
14 may be due to the lower lignin content (which is the most thermally stable
15 compound) in compost compared to lignocellulosic biomass. The third phase
16 (350-600 °C, shoulder in the DTG) to the degradation of aromatic structures and
17 organic polymers such as lignin, or synthesized during the compost stabilization
18 process has been associated (Dhyani et al., 2018; Soobhany et al., 2017).
19 Additionally, the peak found at temperatures above 600 °C to the volatilization of
20 the produced biochar and inorganic components (nitrates and carbonates, etc.)
21 has been attributed (Parthasarathy et al., 2021).

22
23
24
25
26
27
28
29
30
31
32
33
34
35
36
37
38
39
40
41
42
43
44
45
46
47
48
49
50
51
52
53
54
55
56
57
58
59
60
The optimum temperature to obtain the maximum yield will vary depending on
the feedstock. According to the TGA evolution, with a reactor temperature of 450
°C a degradation of the organic matter in the studied composts without
volatilization of the inorganic components can be assured. In this sense, Buah et
al. (2007), Agirre et al. (2013), Ansah et al. (2016) experiences of pyrolysis of
MSW between 400 and 550 °C have carried out and approximately, between

400-600 °C the optimal temperature range for most lignocellulosic materials has been published (Tagade et al., 2021). Nevertheless, within the optimum range, the operating temperature not only modifies the bio-oil yield but also changes its composition. In this regard, it has been published that under lower temperatures more carbon can be produced while, under temperatures between 500 °C and 550 °C, higher bio-oil yields can be found. Also, at temperatures above 600 °C, the bio-oil yield may decrease and an increase of non-condensable gases may be found (Ansari et al., 2018).

3.2. Compost pyrolysis kinetics

Table 2 shows the results of the application of the FWO method. In this regard, Palma et al. (2020) in a study of the pyrolysis of MSW compost, concluded that adjusting the pyrolysis of MSW compost to first-order kinetics appears to be a suitable approach. A similar trend to that found by other researchers in lignocellulosic biomass (Açıklan and Gözke, 2021) has been found in the evolution of the Activation Energy of compost. This similar behavior by other authors has been previously described (Fernández-López et al., 2016). Thus, an increase up to values close to 200 kJ mol⁻¹ has been found at 20% ($\alpha=0.20$) conversion.

Conversion (α)	Ea (kJ mol ⁻¹)	log(A) (log s ⁻¹)
0.2	211.9	20.6
0.3	191.4	19.7
0.4	222.3	20.0
0.5	301.6	21.1
0.6	150.2	21.5
0.7	85.4	23.3

Table 2. Calculated Activation energy of MSWC under conversion degree (α) by using Flynn-Wall-Ozawa method.

The 20% conversion occurs at 300 °C, at this temperature the degradation of hemicelluloses and cellulose begins. In this respect, Collard and Blin (2014) showed that cellulose pyrolytic degradation occurs mainly between 300 and 400 °C. Also, proteins also decompose at such temperatures (Kebelmann et al., 2013). During this process, E_a remains at similar values up to 50% conversion ($\alpha=0.5$), which approximately corresponds to 450°C. At this point, according to Soobhany et al. (2017), with the degradation of aromatic structures, depolymerization of lignin and other organic polymers synthesized during the compost stabilization process (humic and fulvic substances), have been associated and, this fact, can lead to an increase in E_a values to 301.6 kJ mol⁻¹. In this sense, the drop in E_a at the lower values of this parameter for lignin-derived compounds (34.94-122.24 KJ mol⁻¹) (Soh et al., 2019), with respect to those found for cellulosic derivatives (340-360) (Huang et al., 2011), may be due.

The calculated activation energy values are in the range found by other authors (60-600 kJ mol⁻¹) (Fernández-López et al., 2016; Palma et al., 2020). Moreover, Palma et al. (2020) have studied the pyrolysis of MSW compost under two different composting conditions (different aeration and moisture) finding activation energy values in the range of 57.78-581.69 kJ mol⁻¹.

Finally, after the depolymerization processes of the different compounds formed during composting, a drop in E_a has been calculated (to values similar to 150 kJ mol⁻¹) for $\alpha>0.6$, which can be attributed to the volatilization of residual carbon in

1
2
3 the compost (Dhyani et al., 2018) since the temperatures at which it takes place
4 are higher than 600 °C.
5

6
7 The velocity constant, following the Arrhenius Equation (basis of the Flynn-Wall-
8 Ozawa model) can be expressed as (Eq. 2).
9

$$10 \quad k(T) = A \cdot e^{\frac{-E_a}{R \cdot T}} \quad (\text{Eq. 2})$$

11
12 where T is Temperature 450 °C (723 K), R=8.314472 J mol⁻¹ K⁻¹. Substituting the
13 maximum values (Table 2) of Ea (301.6 kJ mol⁻¹) and A (21.1 s⁻¹), we can obtain
14 a velocity constant: k=21.1 mol s⁻¹. Therefore, given the high level of degradation
15 that, under the proposed conditions, takes place. At low material addition levels,
16 to the fluidized bed reactor, a complete conversion can be ensured.
17
18
19
20
21
22
23
24
25

26 **3.3. Material Balance**

27
28 The material was introduced into the pyrolytic reactor at a rate of 1000 g h⁻¹. The
29 operating time was 30 min, thus, 500 g (6% moisture) has been processed.
30
31

32
33 The biochar yields were 83.55 g (16.71 %) and 40.25 g (8.05%) for cyclones CY1
34 and CY2, respectively, with moisture contents of 0.83% and 0.18%, respectively.
35

36
37 This means almost 25% yield in biochar. In this regard, comparable values for
38 different biomasses by Boateng et al. (2012) (17-28%), Jaroenkhasemmesuk
39 and Tippayawong (2015) (30%) and Larina and Zaichenko (2018) (35%), under
40 temperatures similar to the studied ones, have been found. Generally, moisture
41 contents lower than 11% in raw materials have little influence on biochar yield (Di
42 Blasi et al., 2000) because a high initial moisture content of the feedstock and a
43 slow heating rate may result in an incomplete devolatilization of the biochar.
44
45
46
47
48
49
50
51
52

53
54 In the condensable fraction of pyrolysis (pyrolytic liquids), 162.2 g (32.44%) and
55 18.35 g (3.67%) yields in condensers CD1 and CD2, respectively, have been
56 found. This means 36.11% yield in condensable fraction. Comparable values
57
58
59
60

1
2
3 have been found, by Boateng et al. (2012) (10-45%) and Jaroenkhasemmesuk
4 and Tippayawong (2015) (30%) for different biomasses, although lower than
5 those found by Mohan et al. (2006) (60-75%). According to Ferreira (2000),
6 almost 100% of the intrinsic water in the compost (8%) is responsible for the major
7 part and composition of the liquid found in condensers.
8
9

10
11
12
13
14 Over 64% increment in water content with respect to the initial water content has
15 been found. This may be due to the reaction that, at the process temperatures,
16 has been taking place between the oxygenated compounds in the compost (being
17 the product of biooxidative reactions) and the hydrogen released during the
18 pyrolytic degradation reactions, resulting in a high water yield.
19
20
21
22
23
24

25
26 The measured non-condensable gases was 171.6 g (36.32%) with a moisture
27 content of 0.12%. Thus, a total yield in the balance of 95% was calculated. A wide
28 range 27-73% on bibliography (Boateng et al., 2012) have been found because
29 the condensation time and conditions significantly vary the amount of gas
30 produced. In this regard, a value similar to this study by Jaroenkhasemmesuk
31 and Tippayawong (2015) (40%) has been found. Although a value higher than
32 that found by Larina and Zaichenko (2018) (15%) and lower than those found by
33 Mohan et al. (2006) (60-75%), has been calculated. The rest at different process
34 points had to be deposited.
35
36
37
38
39
40
41
42
43
44
45

46 **3.4. Biochar analysis**

47
48 The amount of biochar obtained 35.6 ± 3.2 (w.t.) is slightly higher than that found
49 by Ghorbel et al. (2015) who showed a yield of 31% in biochar from farm breeding
50 compost and similar to the yields obtained in biomass pyrolysis (25-40%) at the
51 reaction temperature (Ghodake et al., 2021). The elemental composition of the
52 resulting biochar in Table 3 is shown. Moreover, the ash content of the resulting
53
54
55
56
57
58
59
60

biochars increased significantly with respect to the feedstock ash due to the loss of organic matter which, during the pyrolysis process, passes into the gas phase. Similarly, the carbon content in the biochar increased by 8.6% with respect to the original compost. The progressive concentration of carbon and minerals during volatilization produced by increasing temperatures can cause this process.

	C (%)	H (%)	O (%)	S (%)
Cyclon 1 (CY1)	46.6 ± 2.7	1.62 ± 0.3	51.2 ± 2.3	0.54 ± 0.1
Cyclon 2 (CY2)	48.7 ± 1.9	1.84 ± 0.5	48.9 ± 2.0	0.51 ± 0.1

^a Mean values and standard deviations were calculated from the triplicates

Table 3. Chemical characteristics of obtained biochar^a.

The H/C and O/C ratios to estimate the stability of biochar in soil are commonly used. O/C ratio may be a suitable indicator of biochar stability and may inform about the general polarity of the material (Shakya and Agarwal, 2017). The O/C ratio the abundance of polar oxygen-containing surface functional groups in biochar can indicate (Rangabhashiyam and Balasubramanian, 2019). Therefore, high values indicate a higher polarity of functional groups. Alternatively, low O/C ratios, because the adsorption mechanism shifts from being mainly based on ion exchange to physisorption (Ahmad et al., 2012), low adsorption capacity may indicate due to the weaker nature of physisorption. In this study, high O/C ratios >0.6 (0.9-1.0) have been found and these data may be indicative of a product that is not very stable in soil and therefore, low stability of the biochar produced can be assumed.

On the other hand, H/C ratio the aromaticity and stability of the biochar (Wei et al., 2020; Xiao et al., 2016) may indicate. Low values for this parameter have been found, therefore a low aromaticity can be shown.

These data, with respect to different biomasses, are shown in Figure 3. Differences, mainly in the H/C ratio, with respect to other biochar have been found. This may be due to the loss of aromatic structures that during composting (Joyce et al., 1998), due to the previous microbiological action, has taken place and that may have caused the differences with respect to other biochar from original biomass.

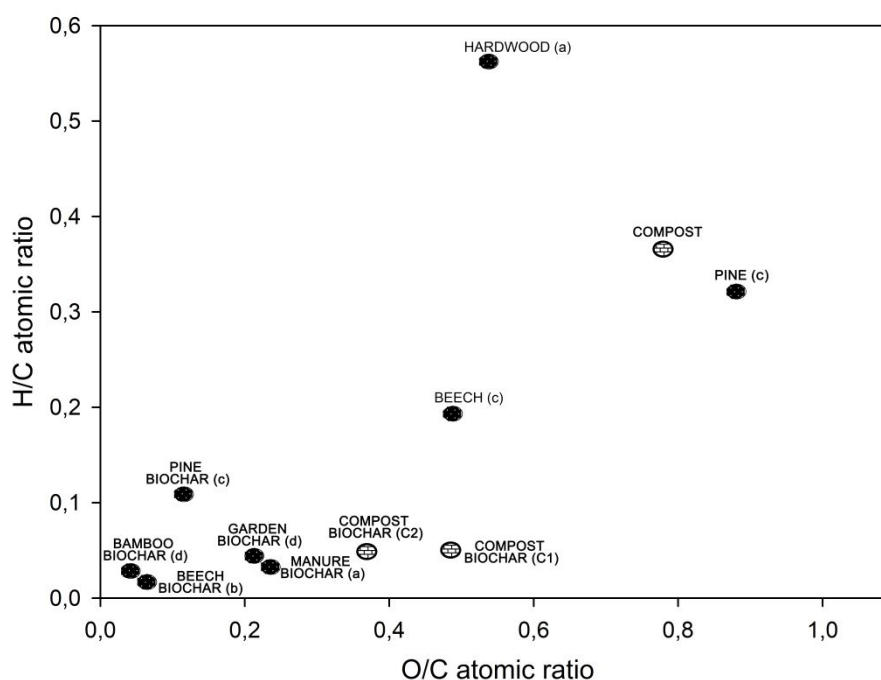


Figure 3. Van Krevelen graph (H/C vs O/C atomic ratio) for the obtained compost biochar with respect to other raw materials (^aFabbri et al. (2012); ^bMorin et al. (2016); ^cGuizani et al. (2017); ^dDang et al. (2021).

Low values of gross heating, 14.18 and 18.56 MJ kg⁻¹ for C1 and C2 samples, respectively, have been found. Values similar to 25-30 MJ kg⁻¹ in biochars from

1
2
3 different feedstocks have been found (Jiang et al., 2018; Tsai et al., 2018), but
4
5 higher than those found by Mierzwa-Hersztek et al. (2019), in the range of 11-12
6
7 MJ kg⁻¹ for sawdust, wheat straw, and miscanthus straw. In this regard, Tripathi
8
9 et al. (2016) showed that the calorific value of biochar is directly proportional to
10
11 the process temperature and inversely proportional to the H/C and O/C molar
12
13 ratios. The obtained data supports the conclusions drawn by these authors.
14
15

16 Alkalinity is one of the most influential properties of biochar, because changes in
17
18 pH have large impact on many soil processes (Fidel et al., 2017). In this study,
19
20 values of 12.04 and 12.37 have been found for C1 and C2, respectively. In this
21
22 regard, Li et al. (2013) and Fidel et al. (2017) showed values between 5.5-10.3
23
24 depending on the biochar feedstock and pyrolysis conditions. The values found
25
26 in biochar from MSW compost, are higher than those found by the previous
27
28 authors. This fact may be due to the high amount of basic salts usually found in
29
30 MSW compost (Xie et al., 2020) that give rise to a basic pH already in the original
31
32 compost and that are concentrated by the pyrolysis process in the biochar
33
34 obtained since the process conditions (450°C) do not cause the volatilization of
35
36 these salts.
37
38
39
40

41 42 **3.5. Bio-oil GC/MS analysis**

43
44 The bio-oil obtained from the pyrolysis of compost at 450 °C for 30 min in a
45
46 fluidized bed reactor was analyzed by GC-MS and are shown in Table 4. Since
47
48 the compost is formed mainly by lignocellulosic material composed of cellulose,
49
50 hemicellulose and lignin, the pyrolysis products are derived from these
51
52 components in different proportions. Numerous chemical compounds have been
53
54 obtained in bio-oils but the complete identification is complex, with 24 of the most
55
56 important compounds identified and studied in depth.
57
58
59
60

The main cellulose decomposition compound in compost pyrolysis as furan-2-ylmethanol (3.3%) and as nitrogenous product is found 5-(hydroxymethyl)-1-methylpyrrolidin-2-one (2.4%) have been found. As shown in Table 4, the phenolic compounds typical in lignin disintegration, such as methylphenols (12.7%), 2-methoxyphenol, better known as guaiacol (6.9%), 4-methylbenzene-1,2-diol (5.7%) or 3-(2-hydroxyethyl)phenol (6.4%) have been found among many others, assuming more than 80% of the total of degraded products.

The low concentration of short-chain compounds common of the fragmentation of cellulose and hemicellulose such as carbohydrates highlighting the levoglucosan in the pyrolytic liquids (Kim et al., 2013) compared to untreated lignocellulosic biomass reveals the decomposition of these components in the composting process, making more complex lignin compounds attract attention to a greater extent.

Compounds	Formula	MS	RT (min)	Area (%)
<i>Ethane-1,2-diol</i>	C ₂ H ₆ O ₂	62.07	12.591	2.45
<i>Furan-2-ylmethanol</i>	C ₅ H ₆ O ₂	98.10	12.904	3.29
<i>Phenol</i>	C ₆ H ₆ O	94.11	14.288	6.32
<i>5-(hydroxymethyl)-1-methylpyrrolidin-2-one</i>	C ₆ H ₁₁ NO ₂	129.16	15.653	2.44
<i>2-methylphenol</i>	C ₇ H ₈ O	108.14	16.050	3.30
<i>3-methylphenol</i>	C ₇ H ₈ O	108.14	16.220	4.58
<i>4-methylphenol</i>	C ₇ H ₈ O	108.14	16.444	4.82
<i>3-methylcyclohex-1-en-1-ol</i>	C ₇ H ₁₂ O	112.17	17.558	6.19
<i>2-methoxyphenol</i>	C ₇ H ₈ O ₂	124.14	18.088	6.29
<i>3-ethylphenol</i>	C ₈ H ₁₀ O	122.16	18.272	2.11
<i>benzene-1,3,5-triol</i>	C ₆ H ₆ O ₃	126.11	19.040	3.08
<i>2-methoxy-5-methylphenol</i>	C ₈ H ₁₀ O ₂	138.16	19.862	3.34
<i>benzene-1,4-diol</i>	C ₆ H ₆ O ₂	110.11	19.938	3.73
<i>3-methylbenzene-1,2-diol</i>	C ₇ H ₈ O ₂	124.12	21.265	2.68
<i>methyl 3-hydroxybenzoate</i>	C ₈ H ₈ O ₃	152.15	21.321	5.36
<i>2,6-dimethoxyphenol</i>	C ₈ H ₁₀ O ₃	154.16	21.450	3.26

<i>4-methylbenzene-1,2-diol</i>	$C_7H_8O_2$	124.14	21.528	5.69
<i>1-(2-hydroxyphenyl)propan-1-one</i>	$C_9H_{10}O_2$	150.17	22.122	5.06
<i>3-(2-hydroxyethyl)phenol</i>	$C_8H_{10}O_2$	138.16	22.528	6.39
<i>2-methoxy-4-propylphenol</i>	$C_{10}H_{14}O_2$	166.22	22.685	4.62
<i>1-(2-hydroxy-6-methoxyphenyl)ethanone</i>	$C_9H_{10}O_3$	166.17	23.553	4.67
<i>2-methoxy-4-prop-2-enylphenol</i>	$C_{10}H_{12}O_2$	164.20	23.861	2.15
<i>1-(4-hydroxy-3-methoxyphenyl)ethanone</i>	$C_9H_{10}O_3$	166.17	24.359	6.01
<i>4-(3-hydroxypropyl)-2-methoxyphenol</i>	$C_{10}H_{14}O_3$	182.22	28.106	2.15

Table 4. Main compounds found by GC/MS in bio-oil of MSW compost pyrolysis at 450°C.

3.6. Non-condensable gases GC/MS analysis

The volatile organic pyrolysis products that are found in a small proportion mixed with mainly nitrogen and other light gases detected by GC/MS are shown in Table 5. In this case, the non-condensable gases contain compounds derived from hemicellulose and cellulose, among other compounds of composted urban waste that barely appeared in pyrolytic liquids.

Compounds	Formula	MS	RT (min)	Area (%)
<i>2-methylpropan-1-ol</i>	$C_4H_{10}O$	74.12	4.140	5.27
<i>1-pentanol</i>	$C_5H_{12}O$	88.15	4.255	4.69
<i>pent-1-en-3-yne</i>	C_5H_6	66.10	4.320	2.93
<i>2-methylpropanal</i>	C_4H_8O	72.11	4.425	3.40
<i>hexanal</i>	$C_6H_{11}O$	100.16	4.660	5.04
<i>2,2-dimethylpropanenitrile</i>	C_5H_9N	83.13	4.965	3.37
<i>(3E)-hexa-1,3,5-triene</i>	C_6H_8	80.13	5.195	5.25
<i>4-methylpenta-1,3-diene</i>	C_6H_{10}	82.14	5.315	3.60
<i>hexa-1,5-diyne</i>	C_6H_6	78.11	5.470	3.82
<i>(3E)-hexa-3,5-dien-2-ol</i>	$C_6H_{10}O$	98.14	5.565	4.04
<i>2,2-dimethylpropanal</i>	$C_5H_{10}O$	86.13	5.935	5.48
<i>2-methylpent-4-en-1-ol</i>	$C_6H_{12}O$	100.16	5.990	2.60
<i>2,5-dimethylfuran</i>	C_6H_8O	96.13	6.130	4.45

<i>(5E)-hepta-1,5-diene</i>	C ₇ H ₁₂	96.17	6.510	3.75
<i>ethenyl acetate</i>	C ₄ H ₆ O ₂	86.09	6.665	4.80
<i>5-methylhexa-1,4-diene</i>	C ₇ H ₁₂	96,17	6.985	5.18
<i>(3E)-2-methylhexa-1,3,5-triene</i>	C ₇ H ₁₀	94.15	7.115	4.64
<i>3-prop-2-enylcyclopentene</i>	C ₈ H ₁₂	108.18	7.270	5.25
<i>(5E)-hepta-1,5-dien-3-yne</i>	C ₇ H ₈	92.14	7.755	4.98
<i>cyclopentanone</i>	C ₅ H ₈ O	84.12	8.340	4.35
<i>octane</i>	C ₈ H ₁₈	114.23	8.595	3.59
<i>methyl 2-methylpropyl carbonate</i>	C ₆ H ₁₂ O ₃	132.16	10.545	2.75
<i>1,3-xylene</i>	C ₈ H ₁₀	106.16	10.715	3.29
<i>1,2-xylene</i>	C ₈ H ₁₀	106.16	10.965	3.47

Table 5. Main compounds found by GC/MS in non-condensable gases of MSW compost pyrolysis at 450°C.

A significant amount of alcohols (16.6%) is found in organic gases, such as 2-methylpropan-1-ol (5.3%), 1-pentanol (4.7%), (3E)-hexa-3,5-dien-2-ol (4.0%) or 2-methylpent-4-en-1-ol (2.6%). There is also a wide variety of aldehydes (13.9%) such as 2-methylpropanal (3.4%), hexanal (5.0%) or 2,2-dimethylpropanal (5.5%). Some compounds derived from hemicellulose and cellulose are also observed, mainly 2,5-dimethylfuran (4.5%). The same compound was also found by Hubble and Goldfarb (2021) in hemicelluloses pyrolytic degradation. A group of compounds derived from plastics and other compounds of more specific urban solid waste can be distinguished, as in the case of 1,3-xylene and 1,2-xylene (3.3% and 3.5%, respectively).

It should be noted that numerous organic compounds with double and triple bonds (36.6%) are obtained from the degradation of carbohydrates, proteins and other typical components of organic matter of animal or human origin (Somorin et al., 2020). The compost has been produced from solid urban waste from

1
2
3 coastal area and is made up of various remains of seashells and bones, so these
4
5 chemical compounds from its decomposition are common.
6

7 8 **4. Conclusions** 9

10 The behaviour of MSW compost and products formed in fluidized bed pilot plant
11 is similar to that established on lignocellulosics raw material. Four characteristic
12 zones (humidity evolution, hemicellulose decomposition, lignin and cellulose
13 degradation and lignin disintegration) have been found.
14
15
16
17

18 The TGA evolution and its kinetic constants similar to those found for
19 lignocellulosic materials have been measured. However, the produced biochar
20 has low stability and aromaticity due to its high and low O/C and H/C ratios,
21 respectively. Additionally, the compounds found in the bio-oil as highly phenolics
22 can be described, it could be due to its humic and fulvic compounds (heavy
23 compounds) in the original material (compost) as well as lignin not degraded
24 during the composting process. Moreover, the compounds in non-condensable
25 gases to thermal degradation of shorter structures such as hemicellulose,
26 proteins and cellulose may be due.
27
28
29
30
31
32
33
34
35
36
37
38
39

40 **Acknowledgments** 41

42 This project (PID2020-112875RB-C21) has been supported by the State
43 Research Agency (SRA - Spanish Ministry of Economy and Competitiveness
44 through the National Programme for Research Aimed at the Challenges of
45 Society) and European Regional Development Fund (ERDF), the Regional
46 Ministry of Innovation, Science and Enterprise, Government of the Junta de
47 Andalucía (Operational Programme FEDER Andalusia 2014-2020. Project UHU-
48 1255540) and research and knowledge transfer micro-projects "Cátedra de la
49
50
51
52
53
54
55
56
57
58
59
60

1
2
3 Provincia", University of Huelva, Spain. Funding for the open access fee is
4 provided by the University of Huelva / CBUA.
5
6

7 **5. References**

8
9
10 Açıkalın K and Gözke, G (2021) Thermogravimetric pyrolysis of onion skins:
11
12 Determination of kinetic and thermodynamic parameters for devolatilization
13
14 stages using the combinations of isoconversional and master plot methods.
15

16 *Bioresource Technology* 342: 125936.
17

18
19 Agirre I, Griessacher T, Rösler G, et al. (2013) Production of charcoal as an
20
21 alternative reducing agent from agricultural residues using a semi-
22
23 continuous semi-pilot scale pyrolysis screw reactor. *Fuel Processing*
24
25 *Technology* 106: 114-121.
26
27

28
29 Ahmad M, Lee SS, Dou X, et al. (2012) Effects of pyrolysis temperature on
30
31 soybean stover- and peanut shell-derived biochar properties and TCE
32
33 adsorption in water. *Bioresource Technology* 118: 536-544.
34

35
36 Ansah E, Wang L and Shahbazi A (2016) Thermogravimetric and calorimetric
37
38 characteristics during co-pyrolysis of municipal solid waste components.
39
40 *Waste Management* 56: 196-206.
41

42
43 Ansari KB, Arora JS, Chew JW, et al. (2018) Effect of Temperature and Transport
44
45 on the Yield and Composition of Pyrolysis-Derived Bio-Oil from Glucose.
46
47 *Energy Fuels* 32(5): 6008-6021.
48

49
50 Baigorri R, Fuentes M, González-Gaitano G, et al. (2009) Complementary
51
52 multianalytical approach to study the distinctive structural features of the
53
54 main humic fractions in solution: Gray humic acid, brown humic acid, and
55
56 fulvic acid. *Journal of Agricultural and Food Chemistry* 57: 3266-3272.
57

58
59 Beis SH, Onay Ö, Koçkar ÖM (2002) Fixed-bed pyrolysis of safflower seed:
60

1
2
3 Influence of pyrolysis parameters on product yields and compositions.
4
5 *Renewable Energy* 26(1): 21-32.
6

7 Boateng AA, Mullen CA, Osgood-Jacobs L, et al. (2012) Mass Balance, Energy,
8 and Exergy Analysis of Bio-Oil Production by Fast Pyrolysis. *Journal of*
9
10 *Energy Resources Technology* 134(4): 042001.
11
12

13
14 Buah WK, Cunliffe AM and Williams PT (2007) Characterization of Products from
15 the Pyrolysis of Municipal Solid Waste. *Process Safety and Environmental*
16
17 *Protection* 85(5): 450-457.
18
19

20
21 Collard FX and Blin J (2014) A review on pyrolysis of biomass constituents:
22 Mechanisms and composition of the products obtained from the conversion
23 of cellulose, hemicelluloses and lignin. *Renewable and Sustainable Energy*
24
25 *Reviews* 38: 594-608.
26
27

28
29 Dang H, Wang G, Wang C, et al. (2021) Comprehensive Study on the Feasibility
30 of Pyrolysis Biomass Char Applied to Blast Furnace Injection and Tuyere
31
32 Simulation Combustion. *ACS Omega* 6(31): 20166-20180.
33
34

35
36 Delgado-Rodríguez M, Ruiz-Montoya M, Giraldez I, et al. (2011) Influence of
37 control parameters in VOCs evolution during MSW trimming residues
38
39 composting. *Journal of Agricultural and Food Chemistry* 59(24): 13035-
40
41 13042.
42
43

44
45 Dhyani V, Kumar M, Wang Q, et al. (2018) Effect of composting on the thermal
46 decomposition behavior and kinetic parameters of pig manure-derived solid
47
48 waste. *Bioresource Technology* 252: 59-65.
49
50

51
52 Di Blasi C, Gonzalez Hernandez E and Santoro A (2000) Radiative Pyrolysis of
53 Single Moist Wood Particles. *Industrial & Engineering Chemistry Research*
54
55 39(4): 873-882.
56
57
58
59
60

- 1
2
3 Díaz MJ, Ruiz-Montoya M, Palma A, et al. (2021) Thermogravimetry applicability
4
5 in compost and composting research: A review. *Applied Sciences* 11(4): 1-
6
7 15.
8
9
10 EEA (2020) Bio-waste in Europe-turning challenges into opportunities. European
11
12 Environment Agency, Report No 04/2020, Denmark.
13
14 El-Sayed SA and Mostafa ME (2015) Kinetic Parameters Determination of
15
16 Biomass Pyrolysis Fuels Using TGA and DTA Techniques. *Waste and*
17
18 *Biomass Valorization* 6: 401-415.
19
20
21 Fabbri D, Torri C and Spokas KA (2012) Analytical pyrolysis of synthetic chars
22
23 derived from biomass with potential agronomic application (biochar).
24
25 Relationships with impacts on microbial carbon dioxide production. *Journal*
26
27 *of Analytical and Applied Pyrolysis* 93: 77-84.
28
29
30 Fachini J, Figueiredo CC, Frazão JJ, et al. (2021) Novel K-enriched
31
32 organomineral fertilizer from sewage sludge-biochar: Chemical, physical and
33
34 mineralogical characterization. *Waste Management* 135: 98-108.
35
36
37 Fernández-López M, Pedrosa-Castro GJ, Valverde JL, et al. (2016) Kinetic
38
39 analysis of manure pyrolysis and combustion processes. *Waste*
40
41 *Management* 58: 230-240.
42
43
44 Ferreira OC (2000) Emissions of greenhouse gases in the production and use of
45
46 plant charcoal. *Revista Economia & Energia* 1: 1-16.
47
48
49 Fidel RB, Laird DA, Thompson ML, et al. (2017) Characterization and
50
51 quantification of biochar alkalinity. *Chemosphere* 167: 367-373.
52
53
54 Finney KN, Ryu C, Sharifi VN, et al. (2009) The reuse of spent mushroom
55
56 compost and coal tailings for energy recovery: Comparison of thermal
57
58 treatment technologies. *Bioresource Technology* 100(1): 310-315.
59
60

- 1
2
3 Flynn JH and Wall LA (1966). General treatment of the thermogravimetry of
4
5 polymers. *Journal of Research of the National Bureau of Standards - A.*
6
7 *Physics and Chemistry* 70A(6): 487-523.
8
9
- 10 Garrido R, Ruiz-Felix MN and Satrio JA (2012) Effects of Hydrolysis and
11
12 Torrefaction on Pyrolysis Product Distribution of Spent Mushroom Compost
13
14 (SMC). *International Journal of Environmental Pollution and Remediation* 1:
15
16 98-103.
17
18
- 19 Ghodake GS, Shinde SK, Kadam AA, et al. (2021) Review on biomass
20
21 feedstocks, pyrolysis mechanism and physicochemical properties of biochar:
22
23 State-of-the-art framework to speed up vision of circular bioeconomy.
24
25 *Journal of Cleaner Production* 297: 126645.
26
27
- 28 Ghorbel L, Rouissi T, Brar SK, et al. (2015) Value-added performance of
29
30 processed cardboard and farm breeding compost by pyrolysis. *Waste*
31
32 *Management* 38: 164-173.
33
34
- 35 Giwa AS, Xu H, Wu J, et al. (2018) Sustainable recycling of residues from the
36
37 food waste (FW) composting plant via pyrolysis: Thermal characterization
38
39 and kinetic studies. *Journal of Cleaner Production* 180: 43-49.
40
41
- 42 Guizani C, Haddad K, Limousy L, et al. (2017) New insights on the structural
43
44 evolution of biomass char upon pyrolysis as revealed by the Raman
45
46 spectroscopy and elemental analysis. *Carbon* 119: 519-521.
47
48
- 49 Gunasee SD, Carrier M, Gorgens JF, et al. (2016) Pyrolysis and combustion of
50
51 municipal solid wastes: Evaluation of synergistic effects using TGA-MS.
52
53 *Journal of Analytical and Applied Pyrolysis* 121: 50-61.
54
55
- 56 Hameed M, Bhat RA, Pandit BA, et al. (2021) Qualitative assessment of compost
57
58 engendered from municipal solid waste and green waste by indexing
59
60

1
2
3 method. *Journal of the Air & Waste Management Association* 72(2): 210-
4
5 219.

6
7 Huang YF, Kuan WH, Chiueh PT, et al. (2011) Pyrolysis of biomass by thermal
8
9 analysis-mass spectrometry (TA-MS). *Bioresource Technology* 102(3):
10
11 3527-3534.

12
13 Hubble AH and Goldfarb JL (2021) Synergistic effects of biomass building blocks
14
15 on pyrolysis gas and bio-oil formation. *Journal of Analytical and Applied*
16
17 *Pyrolysis* 156: 105100.

18
19 Jaroenkhasemmesuk C and Tippayawong N (2015) Technical and Economic
20
21 Analysis of A Biomass Pyrolysis Plant. *Energy Procedia* 79: 950-955.

22
23 Jiang KM, Cheng CG, Ran M, Lu YG (2018) Preparation of a biochar with a high
24
25 calorific value from chestnut shells. *New Carbon Materials* 33(2): 183-187.

26
27 Joyce JF, Sato C, Cardenas R (1998) Composting of polycyclic aromatic
28
29 hydrocarbons in simulated municipal solid waste. *Water Environment*
30
31 *Research* 70(3): 356-361.

32
33 Kebelmann K, Hornung A, Karsten U (2013) Intermediate pyrolysis and product
34
35 identification by TGA and Py-GC/MS of green microalgae and their extracted
36
37 protein and lipid components. *Biomass and Bioenergy* 49: 38-48.

38
39 Kim KH, Kim TS, Lee SM, et al. (2013) Comparison of physicochemical features
40
41 of biooils and biochars produced from various woody biomasses by fast
42
43 pyrolysis. *Renewable Energy* 50: 188-195.

44
45 Larina OM and Zaichenko VM (2018) Thermal cracking in charcoal and ceramics
46
47 of pyrolysis liquid from sewage sludge. *Journal of Physics: Conference*
48
49 *Series* 946: 012034.

50
51 Li M, Liu Q, Guo L, et al. (2013) Cu(II) removal from aqueous solution by *Spartina*
52
53
54
55
56
57
58
59
60

- 1
2
3 alterniflora derived biochar. *Bioresource Technology* 141: 83-88.
4
5 Mierzwa-Hersztek M, Gondek K, Jewiarz M, et al. (2019) Assessment of energy
6 parameters of biomass and biochars, leachability of heavy metals and
7 phytotoxicity of their ashes. *Journal of Material Cycles and Waste*
8 *Management* 21: 786-800.
9
10 Mohan D, Pittman CU and Steele PH (2006) Pyrolysis of Wood/Biomass for Bio-
11 oil: A Critical Review. *Energy Fuels* 20(3): 848-889.
12
13 Morin M, Pécate S, Hémati M, et al. (2016) Pyrolysis of biomass in a batch
14 fluidized bed reactor: Effect of the pyrolysis conditions and the nature of the
15 biomass on the physicochemical properties and the reactivity of char. *Journal*
16 *of Analytical and Applied Pyrolysis* 122: 511-523.
17
18 Ozawa T (1965) A New Method of Analyzing Thermogravimetric Data. *Bulletin of*
19 *the Chemical Society of Japan* 38(11): 1881-1886.
20
21 Palma A, Doña-Grimaldi VM, Ruiz-Montoya M, et al. (2020) MSW compost
22 valorization by pyrolysis: Influence of composting process parameters. *ACS*
23 *Omega* 5(33): 20810-20816.
24
25 Parthasarathy P, Al-Ansari T, Mackey HR, et al. (2021) Effect of heating rate on
26 the pyrolysis of camel manure. *Biomass Conversion Biorefinery* 13: 6023-
27 6035.
28
29 Pietro M and Paola C (2004) Thermal analysis for the evaluation of the organic
30 matter evolution during municipal solid waste aerobic composting process.
31 *Thermochimica Acta* 413 (1-2): 209-214.
32
33 Qian Q, Machida M and Tatsumoto H (2007) Preparation of activated carbons
34 from cattle-manure compost by zinc chloride activation. *Bioresource*
35 *Technology* 98(2): 353-360.
36
37
38
39
40
41
42
43
44
45
46
47
48
49
50
51
52
53
54
55
56
57
58
59
60

- 1
2
3 Rangabhashiyam S and Balasubramanian P (2019) The potential of
4 lignocellulosic biomass precursors for biochar production: Performance,
5 mechanism and wastewater application—A review. *Industrial Crops and*
6 *Products* 128: 405-423.
7
8
9
10
11
12 Rashid MI and Shahzad K (2021) Food waste recycling for compost production
13 and its economic and environmental assessment as circular economy
14 indicators of solid waste management. *Journal of Cleaner Production* 317:
15 128467.
16
17
18
19
20
21 Sánchez-Silva L, Gutiérrez N, Romero A, et al. (2012) Pyrolysis and combustion
22 kinetics of microcapsules containing carbon nanofibers by thermal analysis-
23 mass spectrometry. *Journal of Analytical and Applied Pyrolysis* 94: 246-252.
24
25
26
27
28 Shakya A and Agarwal T (2017) Poultry Litter Biochar: An Approach towards
29 Poultry Litter Management - A Review. *International Journal of Current*
30 *Microbiology and Applied Sciences* 6(10): 2657-2668.
31
32
33
34
35 Soh M, Chew JJ, Liu S, et al. (2019) Comprehensive Kinetic Study on the
36 Pyrolysis and Combustion Behaviours of Five Oil Palm Biomass by
37 Thermogravimetric-Mass Spectrometry (TG-MS) Analyses. *Bioenergy*
38 *Research* 12: 370-387.
39
40
41
42
43
44 Somorin T, Parker A, McAdam E, et al. (2020) Pyrolysis characteristics and
45 kinetics of human faeces, simulant faeces and wood biomass by
46 thermogravimetry-gas chromatography-mass spectrometry methods.
47 *Energy Reports* 6: 3230-3239.
48
49
50
51
52
53 Soobhany N, Gunasee S, Rago YP, et al. (2017) Spectroscopic,
54 thermogravimetric and structural characterization analyses for comparing
55 Municipal Solid Waste composts and vermicomposts stability and maturity.
56
57
58
59
60

1
2
3 *Bioresource Technology* 236: 11-19.
4

5 Tagade A, Kirti N and Sawarkar AN (2021) Pyrolysis of agricultural crop residues:
6 An overview of researches by Indian scientific community. *Bioresource*
7
8 *Technology Reports* 15: 100761.
9
10

11
12 Tripathi M, Sahu JN and Ganesan P (2016) Effect of process parameters on
13 production of biochar from biomass waste through pyrolysis: A review.
14
15 *Renewable and Sustainable Energy Reviews* 55: 467-481.
16
17

18
19 Tsai CH, Tsai WT, Liu SC, et al. (2018) Thermochemical characterization of
20 biochar from cocoa pod husk prepared at low pyrolysis temperature.
21
22 *Biomass Conversion and Biorefinery* 8: 237-243.
23
24

25
26 Wei L, Huang Y, Huang L, et al. (2020) The ratio of H/C is a useful parameter to
27 predict adsorption of the herbicide metolachlor to biochars. *Environmental*
28
29 *Research* 184: 109324.
30
31

32
33 Xiao X, Chen Z and Chen B (2016) H/C atomic ratio as a smart linkage between
34 pyrolytic temperatures, aromatic clusters and sorption properties of biochars
35 derived from diverse precursory materials. *Scientific Reports* 6: 22644.
36
37
38

39
40 Xie K, Hu H, Cao J, et al. (2020) A novel method for salts removal from municipal
41 solid waste incineration fly ash through the molten salt thermal treatment.
42
43 *Chemosphere* 241: 125107.
44
45
46
47
48
49
50
51
52
53
54
55
56
57
58
59
60